AD-A039 375 NAVAL POSTGRADUATE SCHOOL MONTEREY CALIF F/G 13/1
HEAT TRANSFER PERFORMANCE OF VARIOUS ROTATING HEAT PIPES.(U)
DEC 76 L L WAGENSEIL

UNCLASSIFIED NL

1 OF 1
ADA
039375

END

DATE
FILMED
6-77

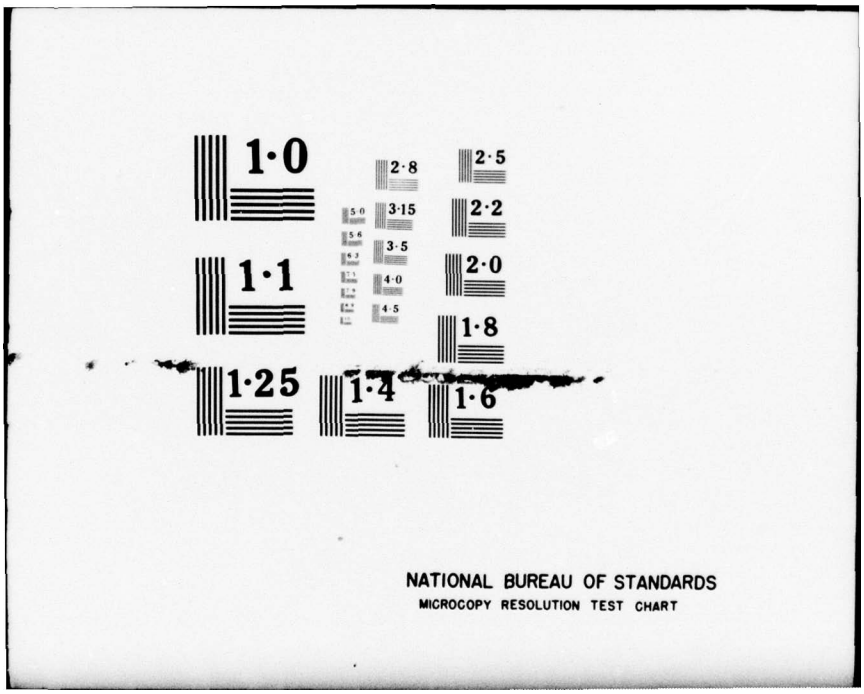
1·0
1·1
1·25
1·4
1·6
1·8
2·0
2·2
2·5
2·8
3·15
3·5
4·0
4·5
5·0
5·6
NATIONAL BUREAU OF STANDARDS
MICROCOPY RESOLUTION TEST CHART

NAVAL POSTGRADUATE SCHOOL
Monterey, California

THESIS

HEAT TRANSFER PERFORMANCE
OF
VARIOUS ROTATING HEAT PIPES

by

Lawrence Lee Wagenseil

December 1976

Thesis Advisor: P. J. Marto

Approved for public release; distribution unlimited.

SECURITY CLASSIFICATION OF THIS PAGE (When Data Entered)

REPORT DOCUMENTATION PAGE

READ INSTRUCTIONS BEFORE COMPLETING FORM

1. REPORT NUMBER

2. GOVT ACCESSION NO.

3. RECIPIENT'S CATALOG NUMBER

4. TITLE (and Subtitle)

(6) Heat Transfer Performance of Various Rotating Heat Pipes,

(9) 5. TYPE OF REPORT & PERIOD COVERED

Master's Thesis, December 1976

6. PERFORMING ORG. REPORT NUMBER

7. AUTHOR(s)

(10) Lawrence Lee Wagenseil

8. CONTRACT OR GRANT NUMBER(s)

9. PERFORMING ORGANIZATION NAME AND ADDRESS

Naval Postgraduate School
Monterey, California 93940

10. PROGRAM ELEMENT, PROJECT, TASK AREA & WORK UNIT NUMBERS

11. CONTROLLING OFFICE NAME AND ADDRESS

(11) Naval Postgraduate School
Monterey, California 93940

12. REPORT DATE

December 1976

13. NUMBER OF PAGES

62

14. MONITORING AGENCY NAME & ADDRESS(if different from Controlling Office)

Naval Postgraduate School
Monterey, California 93940

15. SECURITY CLASS. (of this report)

Unclassified

15a. DECLASSIFICATION/DOWNGRADING SCHEDULE

16. DISTRIBUTION STATEMENT (of this Report)

Approved for public release; distribution unlimited.

(12) 62p.

17. DISTRIBUTION STATEMENT (of the abstract entered in Block 20, if different from Report)

18. SUPPLEMENTARY NOTES

19. KEY WORDS (Continue on reverse side if necessary and identify by block number)

20. ABSTRACT (Continue on reverse side if necessary and identify by block number)

A rotating heat pipe was tested using various copper condenser configurations including two smooth-wall cylinders, an internally finned cylinder and a truncated cone. All condensers were tested with film condensation, and the truncated cone was also tested for dropwise condensation. Each condenser was tested at rotational speeds of 700, 1400 and 2800 RPM with distilled water as the working fluid. → next page

DD FORM 1 JAN 73 1473 (Page 1)

EDITION OF 1 NOV 65 IS OBSOLETE
S/N 0102-014-6601 |

251 450

SECURITY CLASSIFICATION OF THIS PAGE (When Data Entered)

4B

The heat transfer rate of each condenser was plotted against the saturation temperature of the vapor. The main objective was to compare the heat transfer rates obtained with the various condensers in order to identify an optimum configuration for future testing.

In all cases, performance improved with increasing RPM. Dropwise condensation showed substantial improvement in performance relative to film condensation in the same condenser. Similarly, the performance of the internally finned cylindrical condenser was remarkably superior to that of the smooth-wall cylindrical condenser.

Heat Transfer Performance of Various Rotating Heat Pipes

by

Lawrence Lee Wagenseil
Lieutenant Commander, United States Navy
A.B., University of North Carolina, 1966

Submitted in partial fulfillment of the
requirements for the degree of

MASTER OF SCIENCE IN MECHANICAL ENGINEERING

from the
NAVAL POSTGRADUATE SCHOOL
December 1976

Author Lawrence Lee Wagenseil

Approved by: P. J. Marto
Thesis Advisor

Allen E. Fuhs
Chairman, Department of Mechanical Engineering

Robert M. Brown
Dean of Science and Engineering

ABSTRACT

A rotating heat pipe was tested using various copper condenser configurations including two smooth-wall cylinders, an internally finned cylinder and a truncated cone. All condensers were tested with film condensation, and the truncated cone was also tested for dropwise condensation. Each condenser was tested at rotational speeds of 700, 1400 and 2800 RPM with distilled water as the working fluid.

The heat transfer rate of each condenser was plotted against the saturation temperature of the vapor. The main objective was to compare the heat transfer rates obtained with the various condensers in order to identify an optimum configuration for future testing.

In all cases, performance improved with increasing RPM. Dropwise condensation showed substantial improvement in performance relative to film condensation in the same condenser. Similarly, the performance of the internally finned cylindrical condenser was remarkably superior to that of the smooth-wall cylindrical condenser.

TABLE OF CONTENTS

LIST OF TABLES

LIST OF FIGURES

I. INTRODUCTION

A. THE ROTATING HEAT PIPE

The rotating heat pipe is a heat transfer system with potential application for heat removal from rotating machinery. The heat pipe consists of a cylindrical evaporator, a cylindrical or truncated-cone condenser and a working fluid to transport heat between these sections. A heat pipe with a truncated-cone condenser is shown schematically in Figure 1. The heat pipe and auxiliary systems used during this thesis are shown in Figures 2 and 3.

During normal operation the heat pipe is rotated about its longitudinal axis, and the working fluid forms an annulus in the evaporator. Heat input to the evaporator vaporizes some of the working fluid. This vapor fills the evaporator and condenser sections. External cooling is applied to the condenser, and the vapor condenses on the inner wall. Circulation of the working fluid is maintained by the pressure difference between the evaporator and condenser, by the axial component of centrifugal force of rotation acting on the condensate (in the case of the conical condenser) and by the hydrostatic pressure gradient in the condensate (in the case of the right cylindrical condensers).

B. BACKGROUND

The rotating heat pipe used at the Naval Postgraduate School (NPS) initially was designed and constructed in 1970 by Daley [1]. The initial design employed a stainless steel condenser in the shape of a truncated cone with a three degree half-angle. In 1971 Newton [2] conducted experimental work with the basic system. Using the condenser

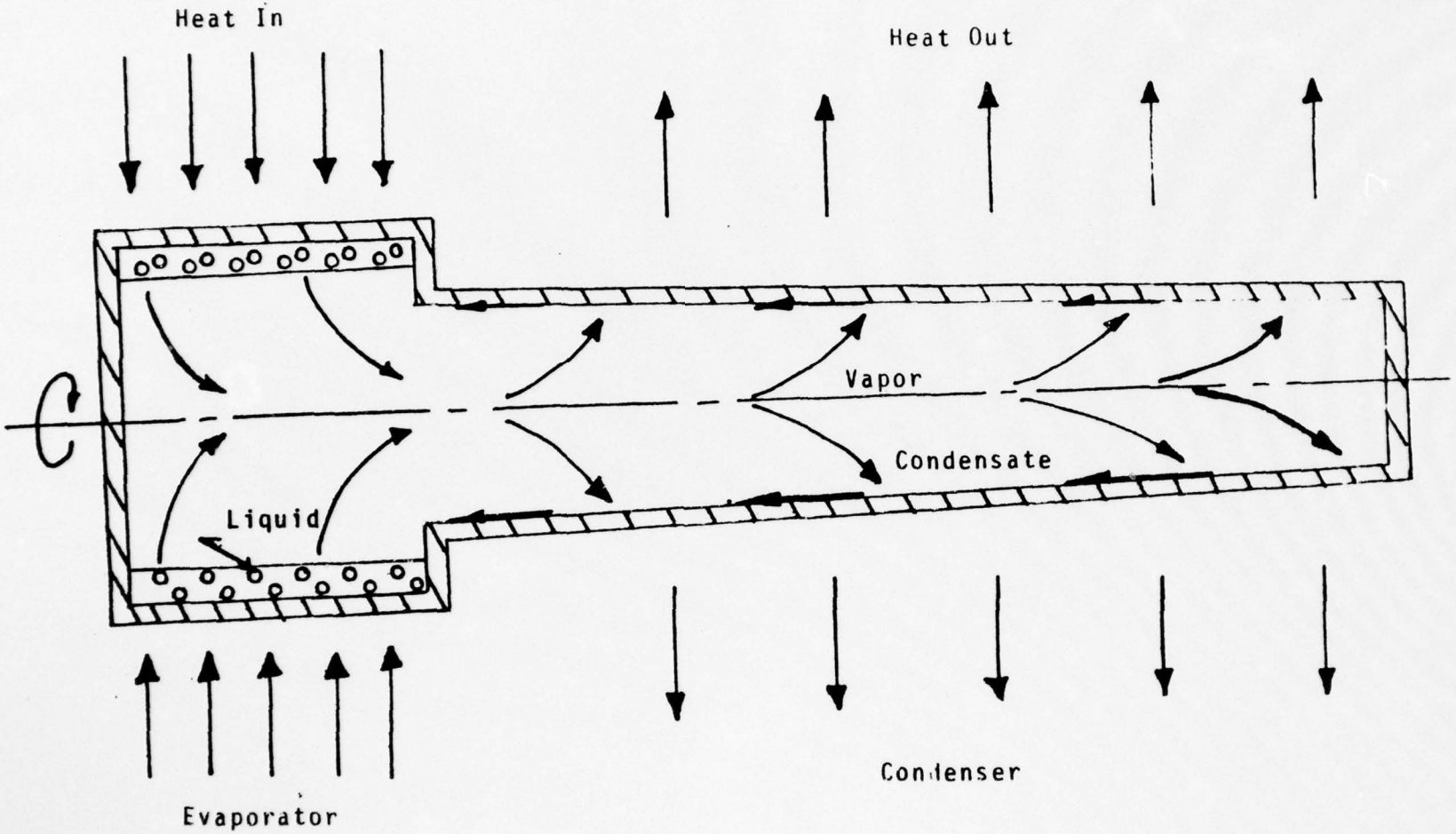

Figure 1. Schematic Drawing of a Rotating Heat Pipe

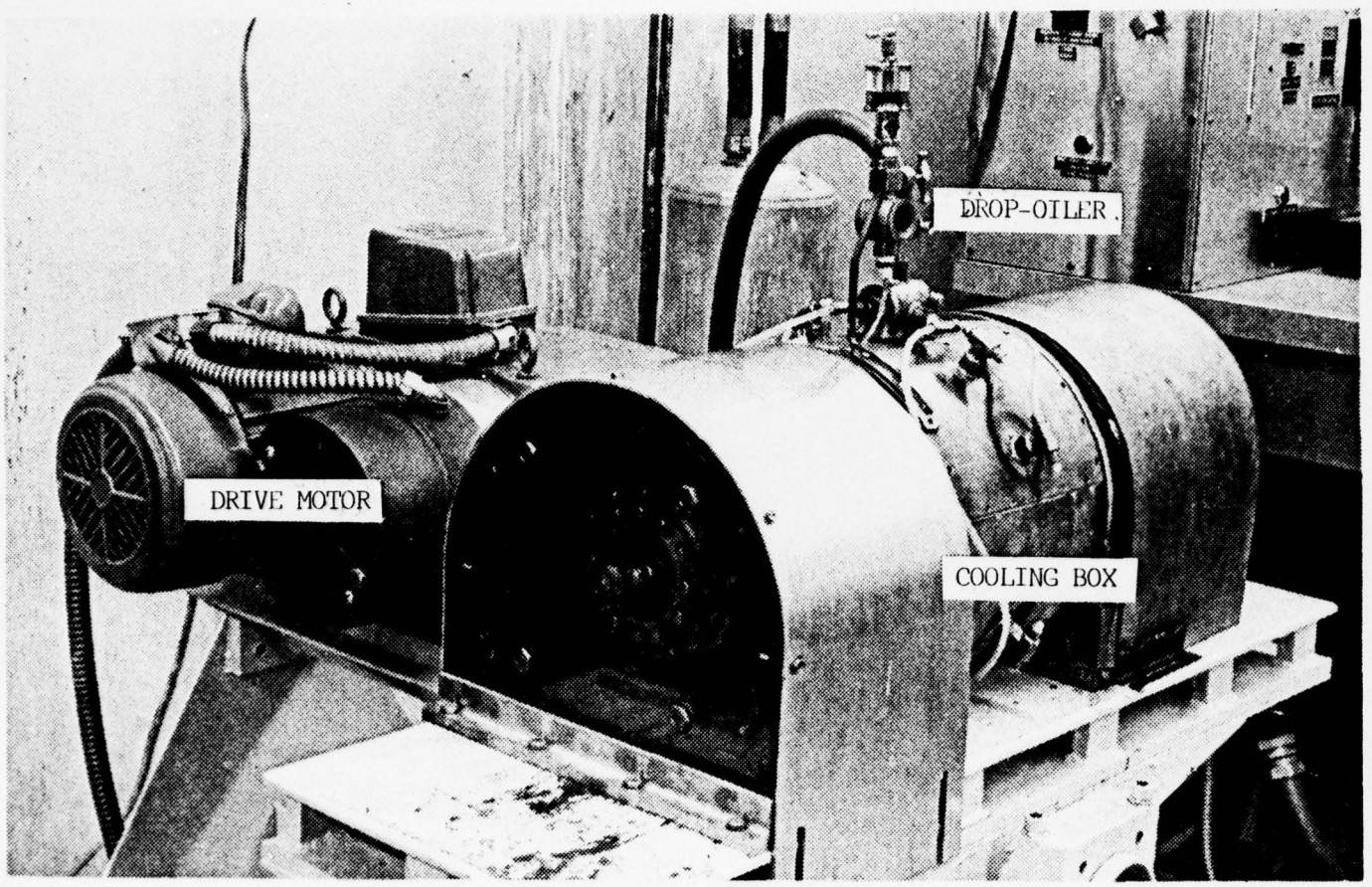

Figure 2. Photograph of the Heat Pipe System in the Running Configuration (with Cooling Box Insulation Removed)

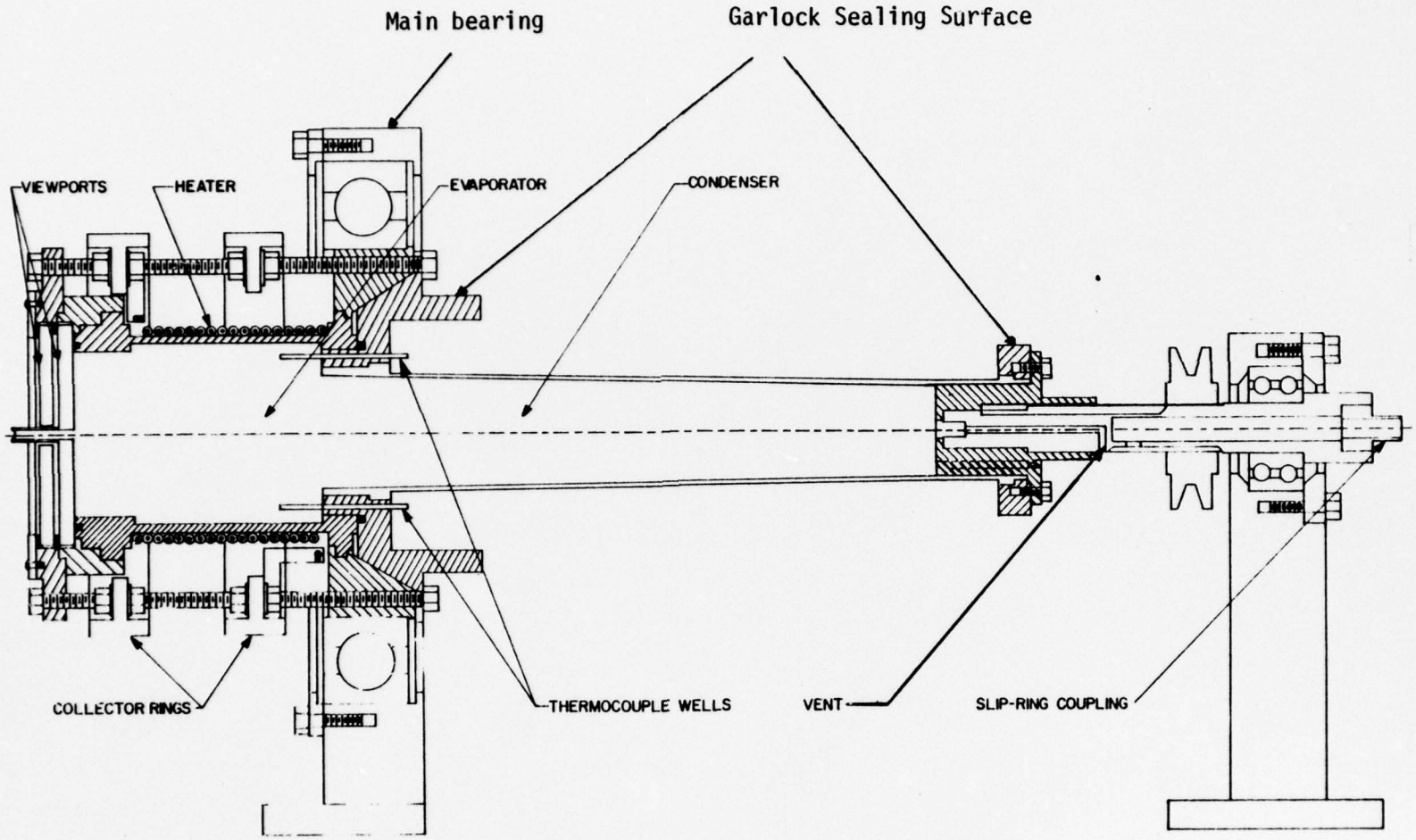

Figure 3. Cross Section Schematic of the Rotating Heat Pipe

from Daley, distilled water as a working fluid and rotational speeds of 702 and 1404 RPM, Newton had the first opportunity to compare analytical and experimental results. In 1972 Woodard [3] continued the research of Newton using the same basic system and working fluid and rotational speeds of 700, 1400 and 2800 RPM. Later that year Schafer [4] expanded the scope of the experimental program. In addition to the stainless steel condenser, a copper condenser of similar geometry was made and tested. Schafer employed various working fluids (alcohol, Freon 113 and water) and used the same rotational speeds as Newton. (These speeds have become standard operational speeds.) In 1974 Tucker [5] continued the research using the copper condenser, standard rotational speeds and various working fluids (water, ethanol and Freon 113). Tucker investigated the effects of the presence of noncondensible gases in the system and attempted to promote dropwise condensation by coating the condenser inner-wall with a silicone grease.

In the course of this intermittent operation of the heat pipe [1-5], several problem areas had been recognized. Solutions to the major problems were known, and in 1976 Loynes [6] redesigned parts of the system incorporating these improvements. Loynes ran the heat pipe and obtained results similar to those of Tucker.

C. THESIS OBJECTIVES

The objectives of this thesis were two-fold:

1) to make additional mechanical improvements to the system in order to improve the reliability, ease of operation and system flexibility, and
2) to experiment with several different condensers in an attempt to select an optimum geometry for additional research.

II. EXPERIMENTAL EQUIPMENT

A. DESCRIPTION OF EQUIPMENT

1. Evaporator

The cylindrical copper evaporator (Figure 4) with O-ring seals at each end, as developed by Loynes [6], was used throughout the thesis without change and proved to be satisfactory.

2. Heater

The heater is a resistance heating element wrapped around the evaporator as shown in Figure 4. The heater was reinsulated at the beginning of this thesis by applying two layers of Sauereisen cement over the heater. A quilted insulating pad was taped around the heater and then wrapped with 0.25 inch wide woven nylon tape. This wrapping was secured in three places by wires passed over the nylon and twisted tightly. This insulation did not fail during subsequent operation.

3. Power Supply

The solid state phase amplifier power controller used by Loynes [6] performed erratically during the initial stage os this investigation. This problem was made manifest by sudden and large (five to ten volts) fluctuations on the control panel voltmeter and was overcome by using a six-volt battery as a power supply for the controller circuit of the silicon controlled rectifier of the system.

4. Heat Pipe Vent

Tucker [5] drilled a 0.125 inch diameter vent hole through the condenser end-plug (Figures 3 and 5). The hole reduced to a smaller diameter just before penetrating the evaporator end of the plug, leaving a shoulder on which an O-ring could be seated. The larger hole was

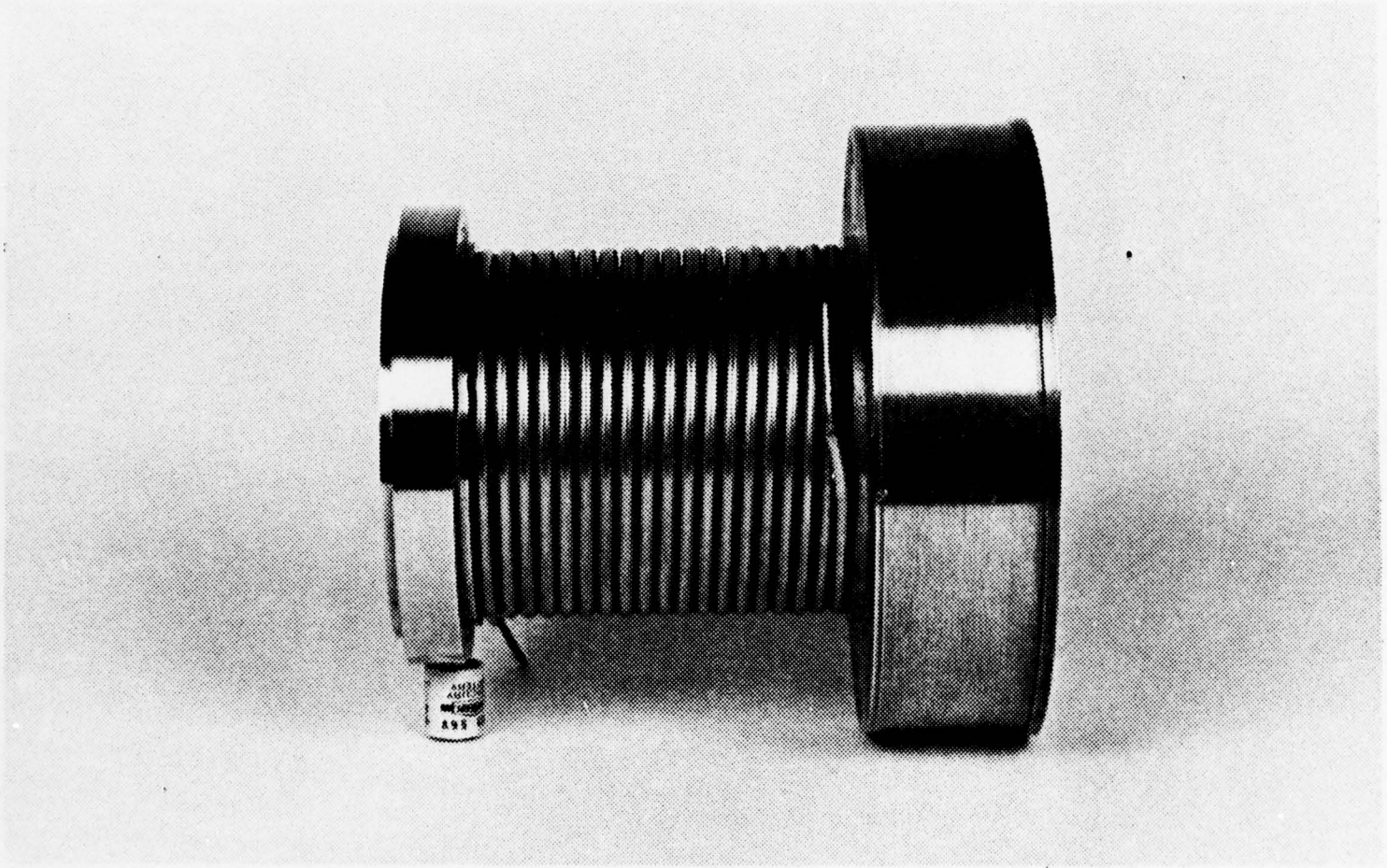

Figure 4. Photograph of the Evaporator and Heater

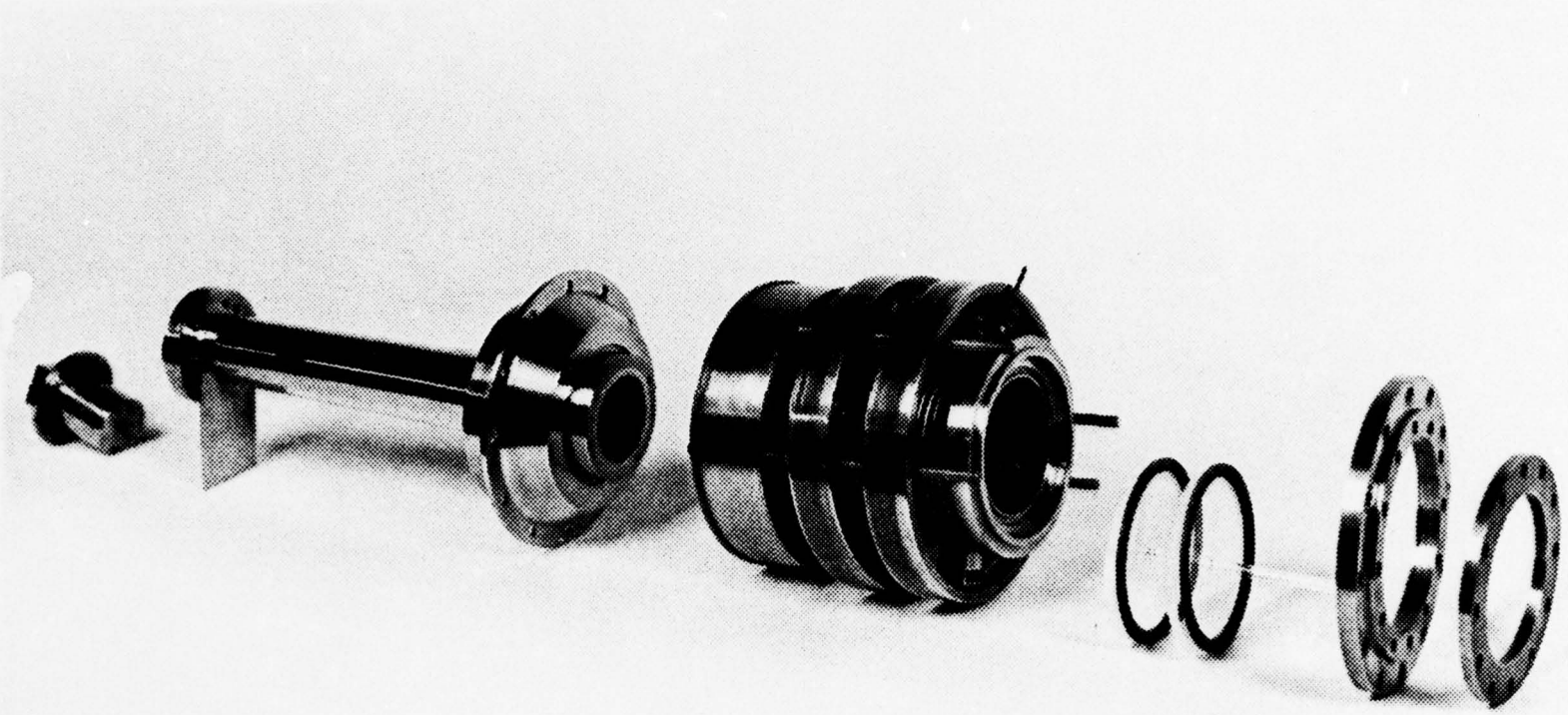

Figure 5. Photograph of the Rotating Heat Pipe (with Glass Fill Tube instead of Copper Tube Actually Used)

threaded and a screw used to seat the O-ring. However, positive control of the vent screw was difficult in this configuration, and this vent hole was silver-soldered shut. A replacement vent hole was then drilled down the center of the drive shaft (Figure 3). This hole stopped just short of the hole bored from the other end for passage of the thermocouple leads. Another hole was drilled along the shaft radius until it intersected the axial hole. This radial passage was tapped for the vent screw and O-ring used by Tucker.

5. View Pieces and Filling Tube

Since the incorporation by Newton [2] of a one-piece glass window and filling tube, this design has been used for all further research. For the resumption of work by Loynes [6], additional end pieces were made by a local commercial glass worker. These proved to be faulty, and all of them failed by cracking circumferentially. Therefore, for this thesis a polycarbonate material was used as the view pieces. The inner piece (Figure 5) was drilled and tapped in the center for a 0.375 inch pipe, and a brass SWAGELOCK fitting was installed. A 6.0 inch long 0.25 inch diameter copper tube was installed in this fitting and used for evacuation and filling (discussed below). The polycarbonate does not afford the same transparency as the glass and scratches easily. Other problems resulted and are discussed in the section on operation.

6. Heat Pipe Balancing

When operation was resumed after the work by Loynes [6] and the heat pipe was reassembled after the insulation was replaced, large magnitude vibration of the system was observed at about 1050 RPM. It was possible to pass through this speed and operate at 1400 RPM. The vibration became severe at about 2100 RPM, and the highest operational speed of 2800 RPM could not be achieved. The need to balance dynamically the

assembled system was obvious. This was accomplished readily by using the NPS Tinius Olsen type E-O horizontal dynamic balancing machine. A solid aluminum bar was machined to fit in the vibratory cradle, and the bar was drilled and tapped to receive the bolts used to bolt the main bearing housing to the test stand. Coupling of the heat pipe to the balancing machine was accomplished using an old heat pipe drive shaft drilled and tapped to permit attachment of the standard balancing machine drive adapter. After the bar was mounted and clamped to the vibratory cradle, balancing was accomplished easily.

After reassembly of the heat pipe, the system was run over its operating range and performed very smoothly at all speeds.

7. Heat Pipe Lubrication

During all previous operations, the lubrication of the main bearing (Figure 3) had followed the procedure established by Woodard [3], that is, applying oil to the bearing prior to a run by squirting it into a tube that emptied over the bearing race. For long periods of operation, the operator added oil as was considered necessary. However, during the balancing of the system, as noted above, the need for continuous lubrication was ascertained. While turning the assembly on the balancing machine, bearing noise (hidden during normal running) and an increase in magnitude of the amount of imbalance (as indicated on the d.c. microammeter) were observed to occur within a few seconds after applying a few drops of oil to the bearing.

Therefore, upon reinstallation on the heat pipe test stand, a small drop-oiler (Figure 2) was installed over the main bearing housing. This unit consisted of a small reservoir with a needle valve for flow regulation. A sight glass permitted observation of the flow from the

reservoir. A flow rate of one drop every 20-30 seconds was found to be adequate. The capacity of the reservoir was adequate to last for several hours of operation. Drain holes in the base of the bearing housing were plugged, and an oil-proof gasket material was placed on each side of the bearing in order to contain the oil and maintain an oil reservoir at the bottom of the bearing, as is standard with ball bearing lubrication.

8. Condenser Modifications

In pursuit of the first objective, several major modifications were made to the condenser section.

The condensers used in past research [1-6] had both end pieces permanently attached. This necessitated production of a new condenser-to-evaporator end-piece for each new condenser. To enable the use of the same condenser-to-evaporator end-piece (hereafter, the main condenser flange or main flange), a new main flange was manufactured with a recess 0.10 inch deep and 3.60 inches in diameter machined into the condenser-side face. The recess was drilled and tapped for eight screws, and an O-ring groove was cut on a radius inside the screw holes. Smaller adaptor flanges were then made that were permanently attached to each individual condenser by silver-soldering. These flanges were drilled to permit attachment to the main flange by bolting. The smaller condenser flange has a 0.90 inch long sleeve over the outside of the condenser. The thickness of this sleeve can be varied by altering the inside diameter to permit use of various condenser (outside) diameters. The sleeve fits snugly into the center hole of the main flange. Figure 6 shows a main flange (without thermocouples) and one of the small condensers with the adaptor flange in place.

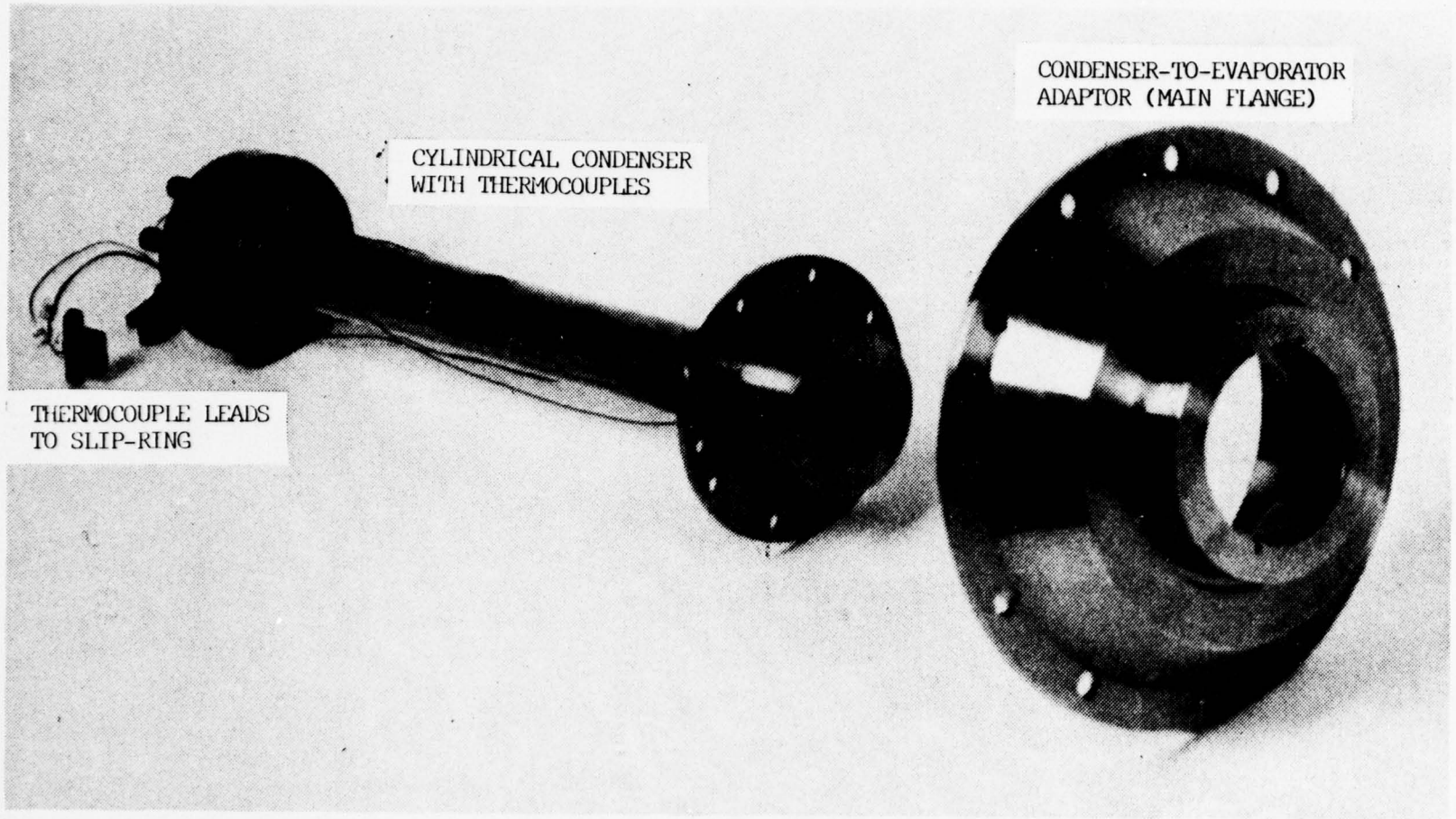

Figure 6. Photograph of the Condensor-to-Evaporator Adaptor with Cylindrical Condenser

To accommodate the various condenser inside diameters, the end plug (Figure 5) was machined to an outside diameter of 0.990 inch. Over this basic plug a cylindrical sleeve was attached by set screws. The sleeve outside diameter was machined to fit the different condensers. An O-ring was used to provide the seal between the condenser and end plug.

Four condenser geometries were selected for testing. These were the standard truncated cone with one degree half-angle, two cylinders with inside diameters of 1.000 and 1.460 inches and an internally finned condenser described below. The truncated cone had a one inch long section that was cylindrical so that the end plug could be inserted. The inside diameter of this section was 1.460 inches. This dimension set the size of the larger cylindrical condenser. The dimensions of the smaller cylindrical condenser were chosen to match the size (inside diameter and wall thickness) of the internally finned condenser. Condenser wall thickness was 0.0625 inch for the cone and large cylinder and 0.030 inch for the small cylinder and finned condenser.

The internally finned condenser was fabricated from a tube furnished by Noranda Metal Industries, Inc., of Newton, Connecticut. The tube specifications are given in Table I. The area ratio of this tube to one of equal diameter without fins is 1.64. Figure 7 is a photograph of the internally finned condenser.

TABLE I. Specifications of the Internally Finned Tube

Number of fins	16
Outside diameter	1.050 inches
Inside diameter	0.999 inch
Fin height	0.084
Unfinned wall area	0.150 ft^2/ft length
Finned area	0.280 ft^2/ft length
Fin spacing	0.143 inch
Fin pitch	6.0 inches (left-hand twist)

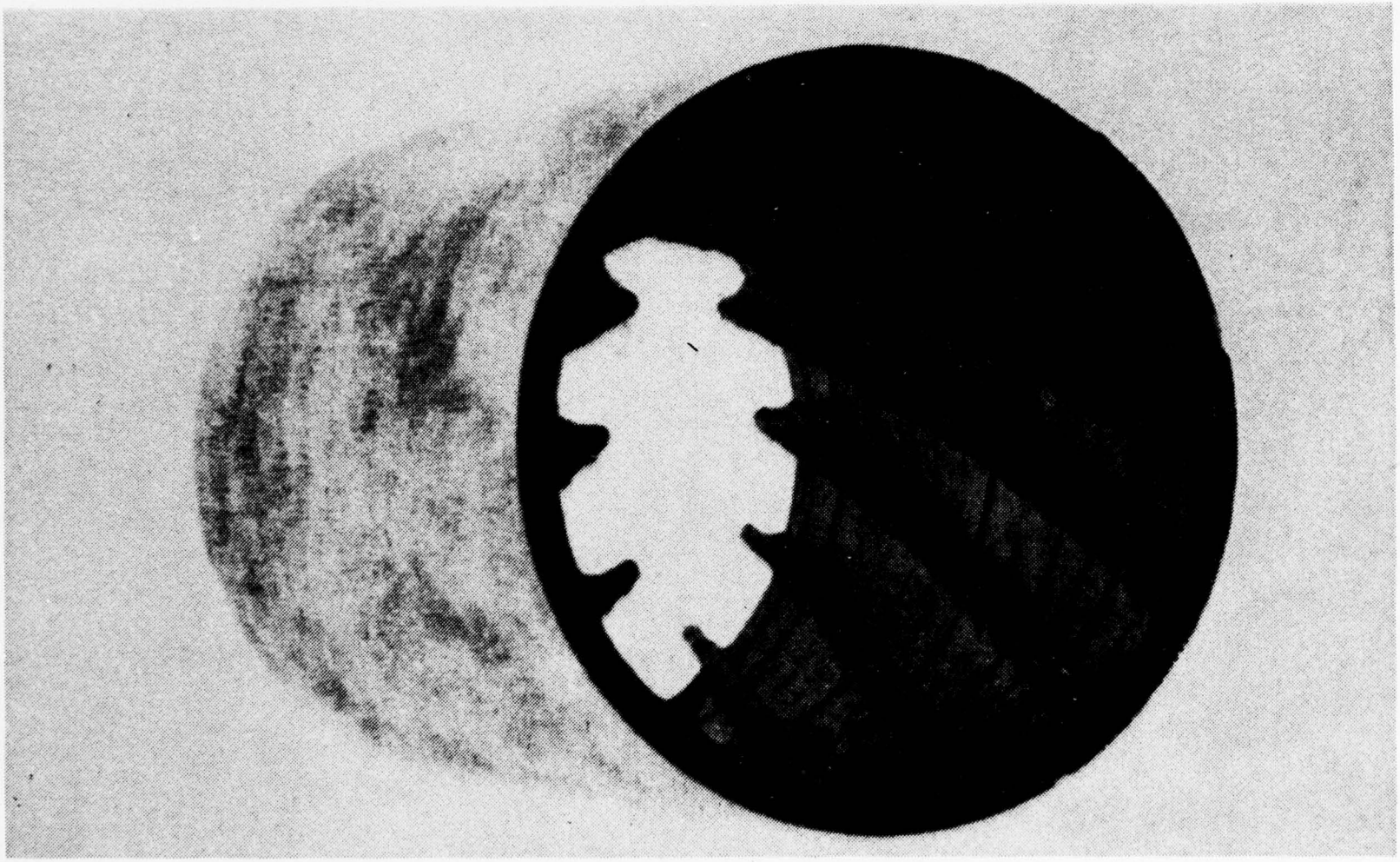

Figure 7. Photograph of a Section of the Internally Finned Condenser.

9. Heat Pipe Drive System

To ensure safe operation with the thin-walled condensers, the mechanical brake on the drive motor, Figure 2, was disconnected. Consequently, when power to the motor was secured, stopping of the heat pipe was accomplished by friction of rotation; this eliminated the danger of excessive torque being applied to the condenser wall.

10. Evacuation and Filling System

The basic evacuation and filling system and procedure were established by Woodard [3]. The filling system utilized for this thesis consisted of three high vacuum valves, a mercury manometer, a 1000 milliliter round bottom flask, a liquid nitrogen cold trap, associated tubing and both mechanical and diffusion vacuum pumps, as shown schematically in Figure 8. The operational procedure and performance of the system are discussed below.

11. Cooling System

The condenser wall temperature profile given by Tucker [5] showed high temperatures at each end of the condenser and much lower, but not constant, temperatures in the middle. In an effort to flatten the wall temperature profile, and thereby achieve a more predictable heat flux, Loynes [6] replaced Tucker's spray cooling system with a direct impingement cooling system. This system, shown schematically in Figure 9, was used throughout this thesis. The four supply tubes are 0.25 inch diameter copper tubes with 0.03125 (1/32) inch holes drilled every 0.20 inch. The supply tubes run the length of the condenser, parallel to the axis. Filtered and 'softened' tap water is used as the cooling fluid. The cooling system is contained in a sealed and insulated box, as shown in Figure 2 (with the outer insulation removed). The

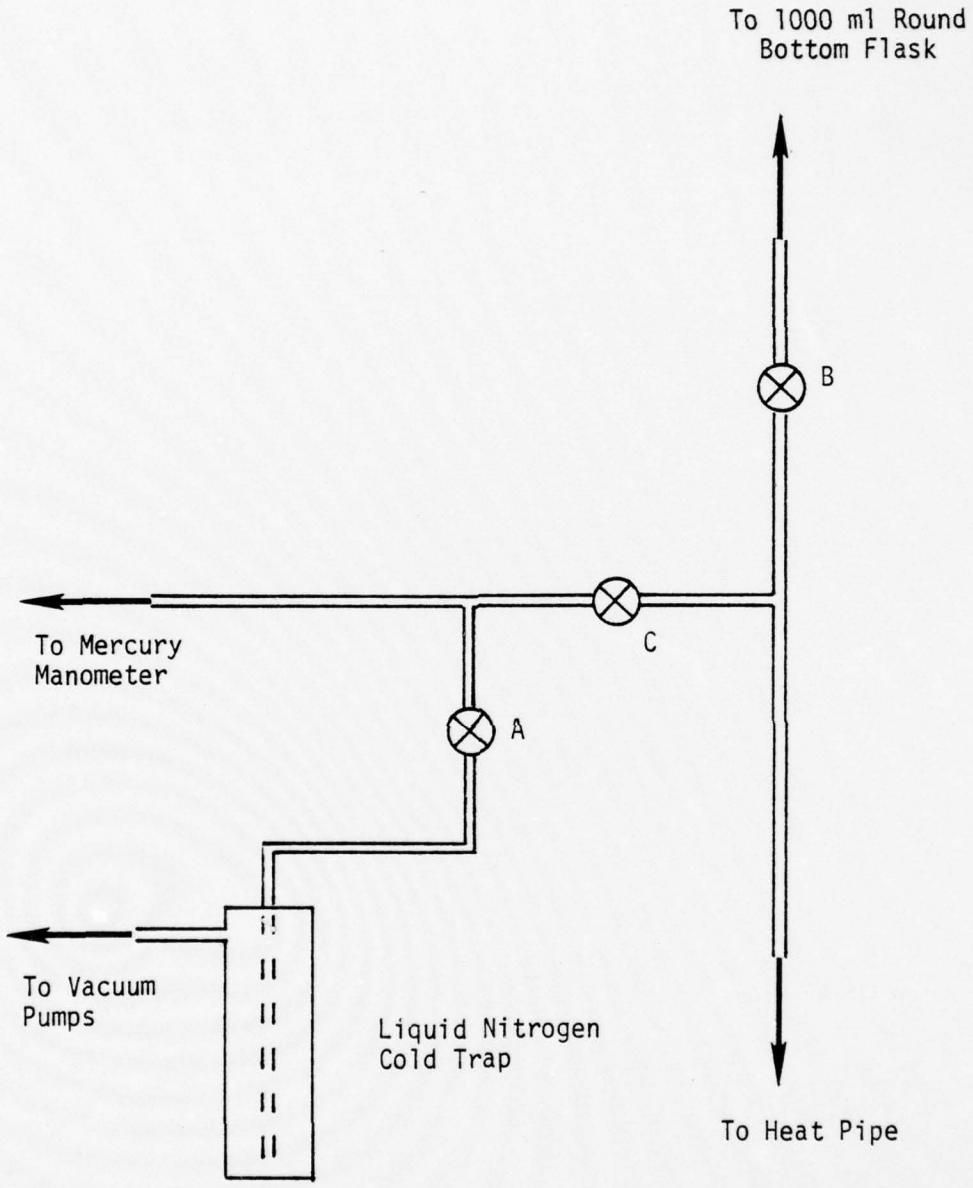

Figure 8. Schematic Drawing of the Evacuation and Fill System

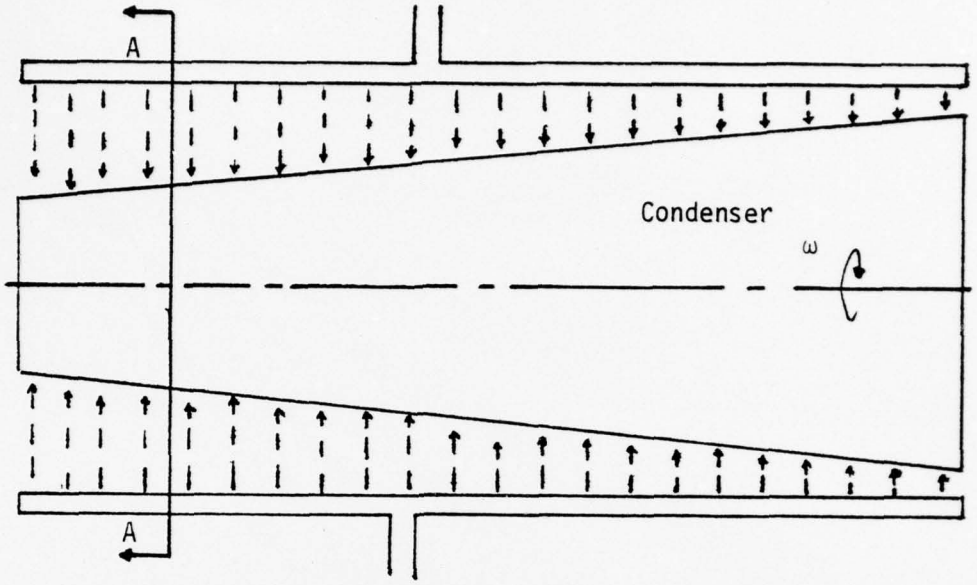

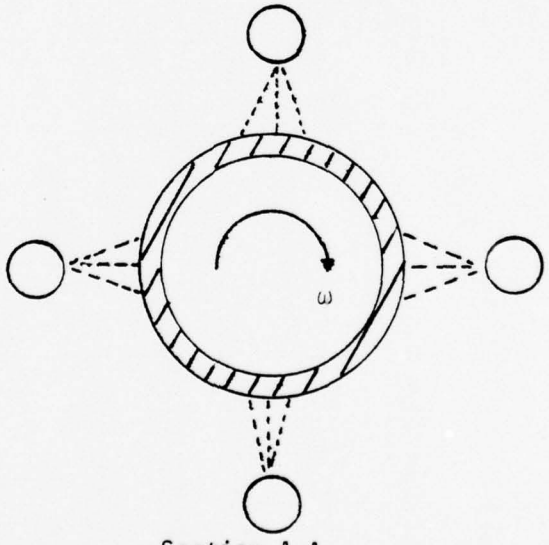

Figure 9. Cooling System Schematic

condenser is rotated inside this box, water containment being maintained by Garlock seals mating with the flanges on either end of the condenser. Figure 10(a,b,c) shows the condenser and cooling system inside the cooling box.

B. INSTRUMENTATION

The condenser instrumentation used by Tucker [5] and shown in Figures 6 and 11 consisted of nine copper-constantan thermocouples. The truncated-cone condenser had Kapton insulated wires. The Kapton had a tendency to crack at sharp bends and ultimately the wires broke at these bends. Because the operating temperatures of the condenser wall and evaporator were well below the maximum sustainable temperature of teflon insulation, all subsequent condensers were instrumented with teflon-insulated wires. These proved to be very flexible and are not likely to break as a result of bending.

Nine grooves were machined in the condenser wall as shown in Figure 11. The groove depth was 0.010 inch for the thin-walled condensers and 0.025 inch for the thick-walled condensers. The welded thermocouple beads were soldered into the grooves with a standard lead-tin low temperature solder. The leads were secured to the condenser by banding with twisted wire and were passed through the small condenser flange, as shown in Figure 6 (with some of the securing wires removed), to mercury slip-rings on the test stand.

Two additional thermocouples penetrated the main flange, sheathed in 0.0625 inch stainless steel tubing. The sheaths protruded two inches into the evaporator to measure the vapor temperature and were soldered closed at the tip to maintain the system vacuum.

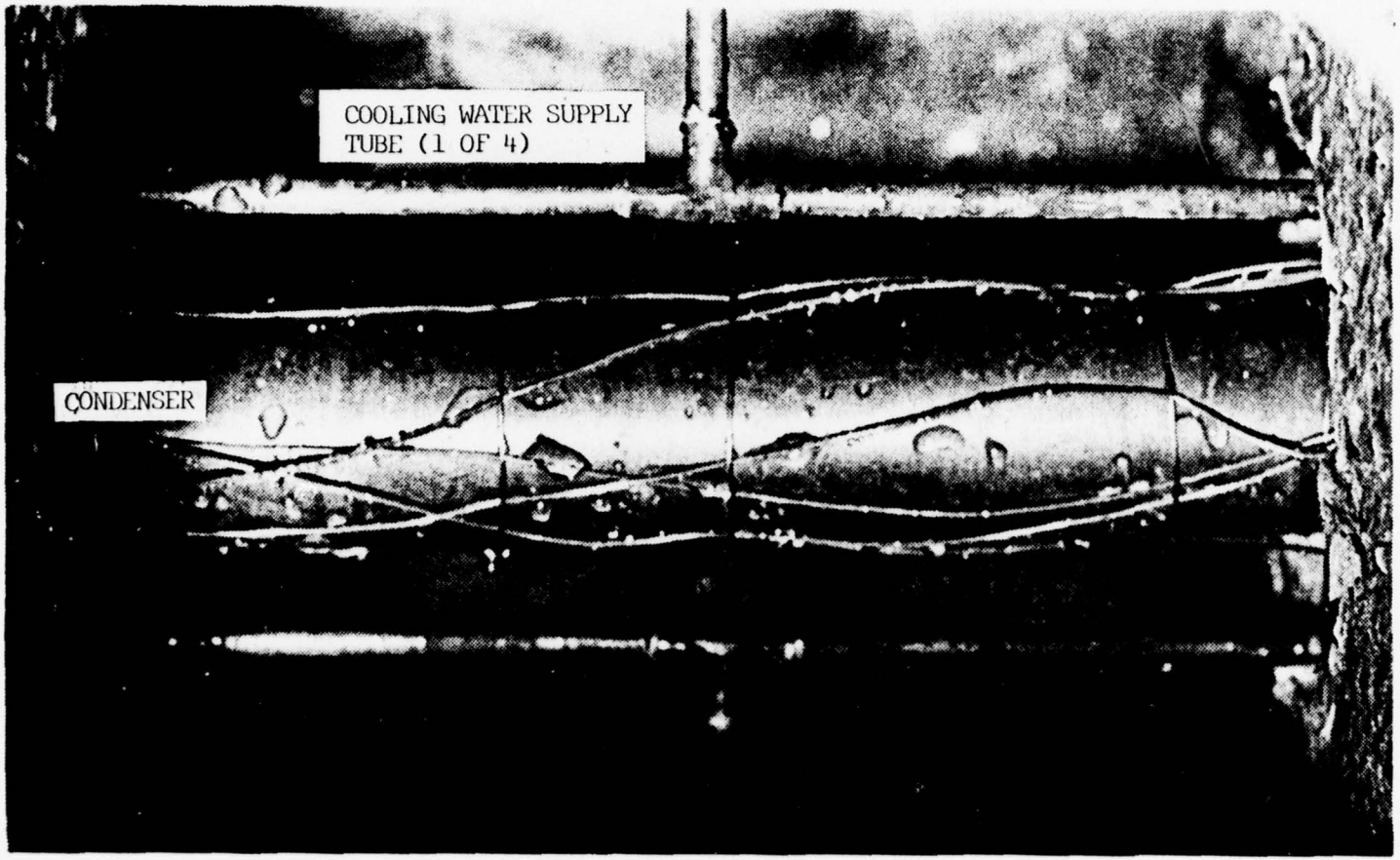

Figure 10(a). Close-up View of Cooling System and Condenser

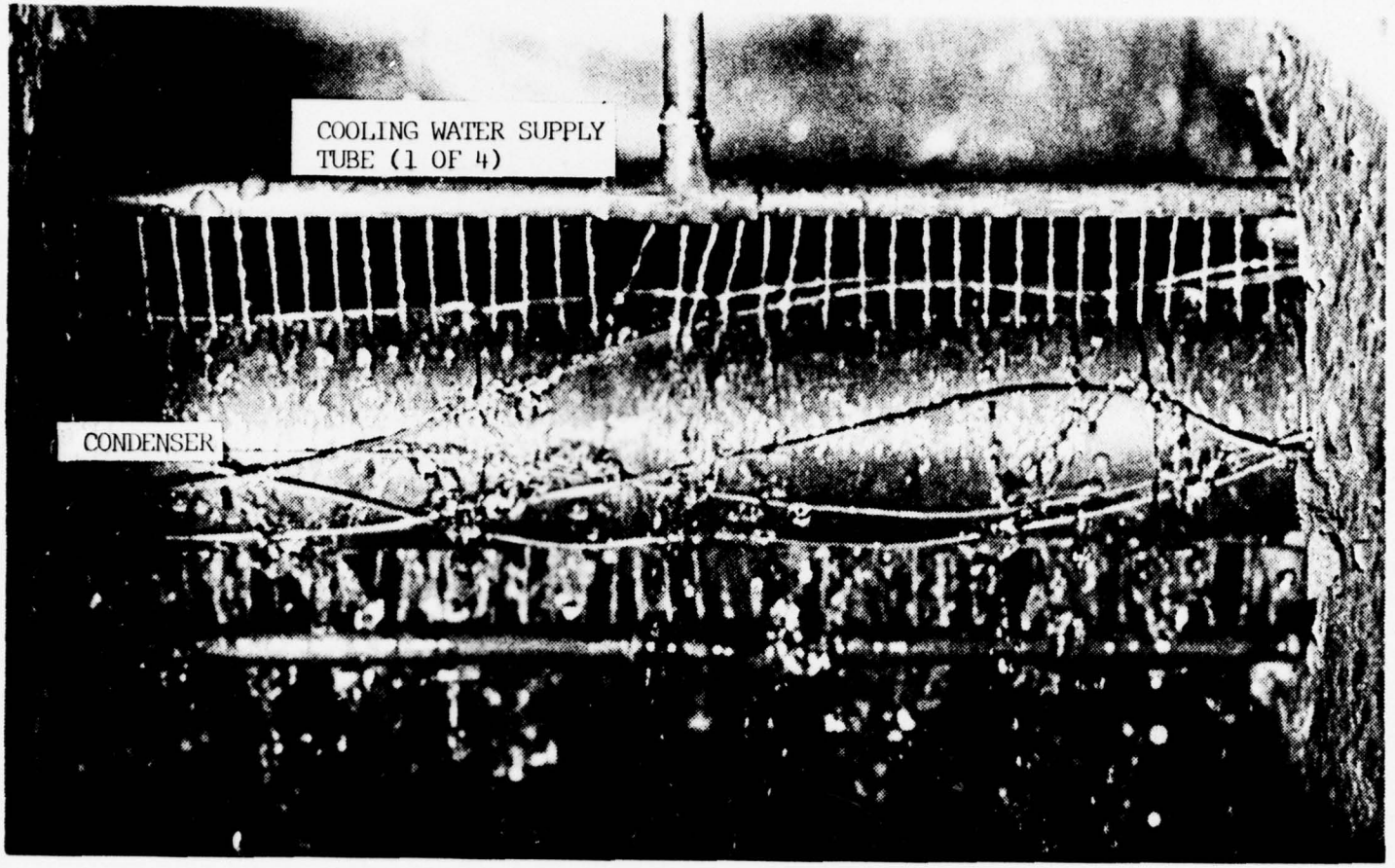

Figure 10(b). Close-up View of Non-rotating Condenser with Cooling Water Flowing at 40 Percent of Maximum Flow

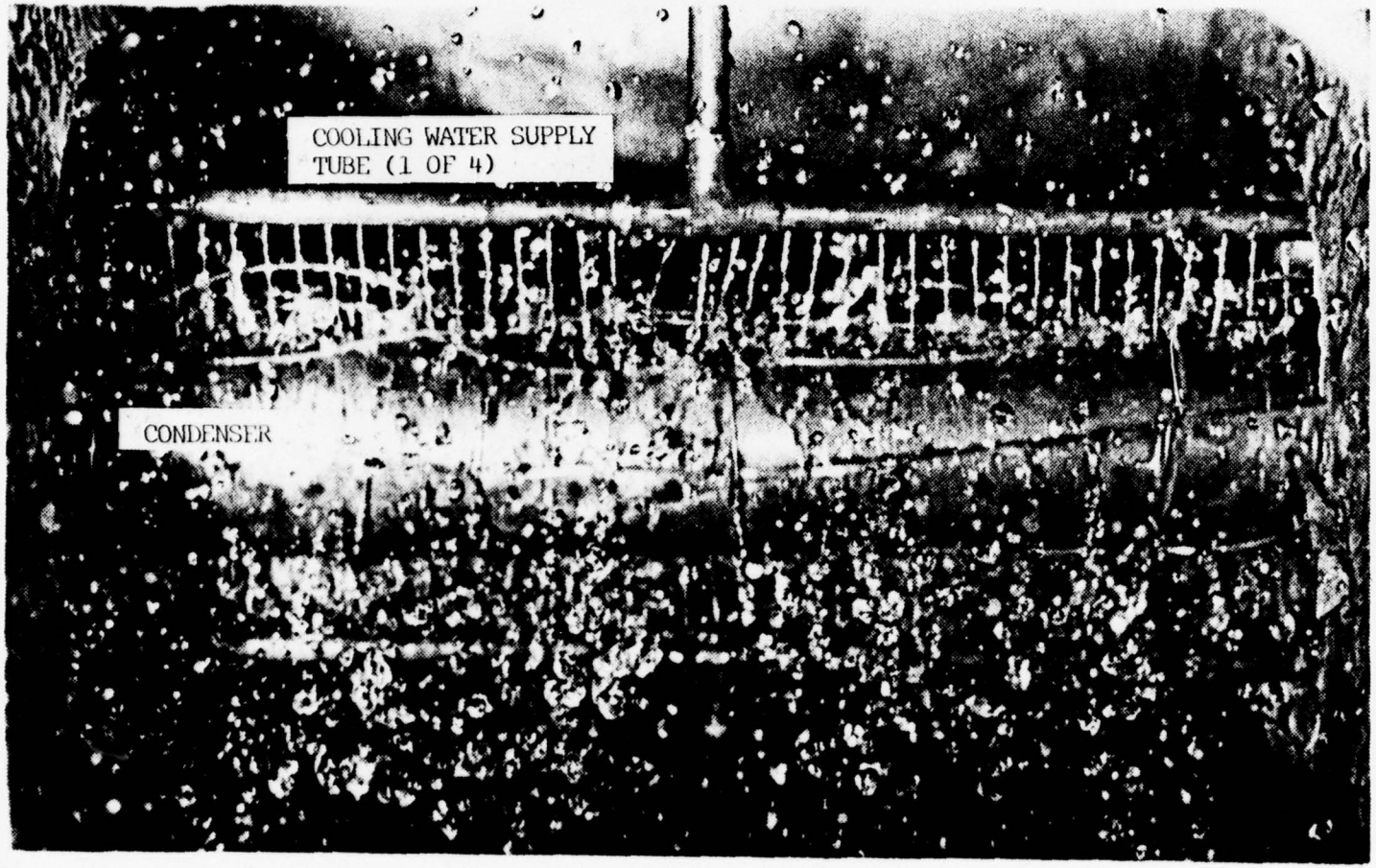

Figure 10(c). Close-up View of Condenser Rotating at 700 RPM and Cooling Water Flowing at 40 Percent of Maximum Flow.

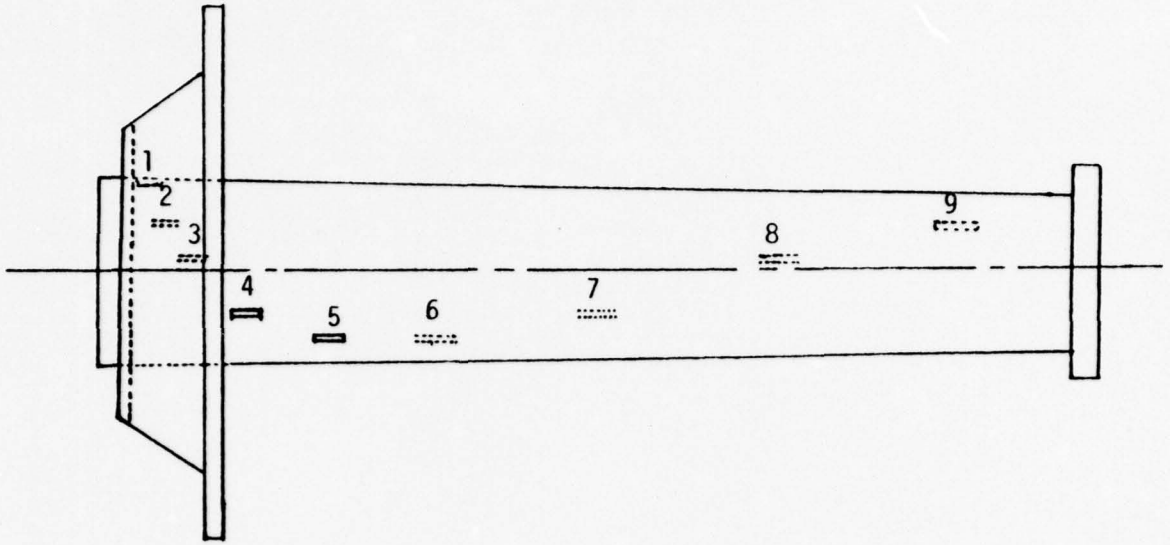

Thermocouple Number	Distance from Evaporator Wall, inches
1	0.20
2	0.35
3	0.60
4	1.00
5	2.00
6	3.00
7	5.00
8	7.00
9	9.00

Figure 11. Schematic View of Thermocouple Positions on the Condenser Wall

The inlet and outlet temperature of the cooling water was monitored by Kapton insulated copper-constantan thermocouples. The outlet thermocouple was actually five separate thermocouples wired in parallel and inserted into the outlet mixing box discharge line, Figure 12.

The condenser-mounted thermocouples were wired into connectors as shown in Figure 6. These mated with the connectors of the slip-ring leads. During operation, the connectors and leads were taped and wired to the drive shaft. The slip-ring channel leads, as well as the cooling water inlet and outlet temperature thermocouples, were wired directly to a Hewlett Packard model 2010C data acquisition system.

Cooling water flow rate was measured with a standard rotameter. Accurate regulation of the flow rate was accomplished by adjusting the pressure regulator installed in the cooling line. This regulator, when cleaned, provided flow rates easily maintained to within $\pm$ 0.50 percent.

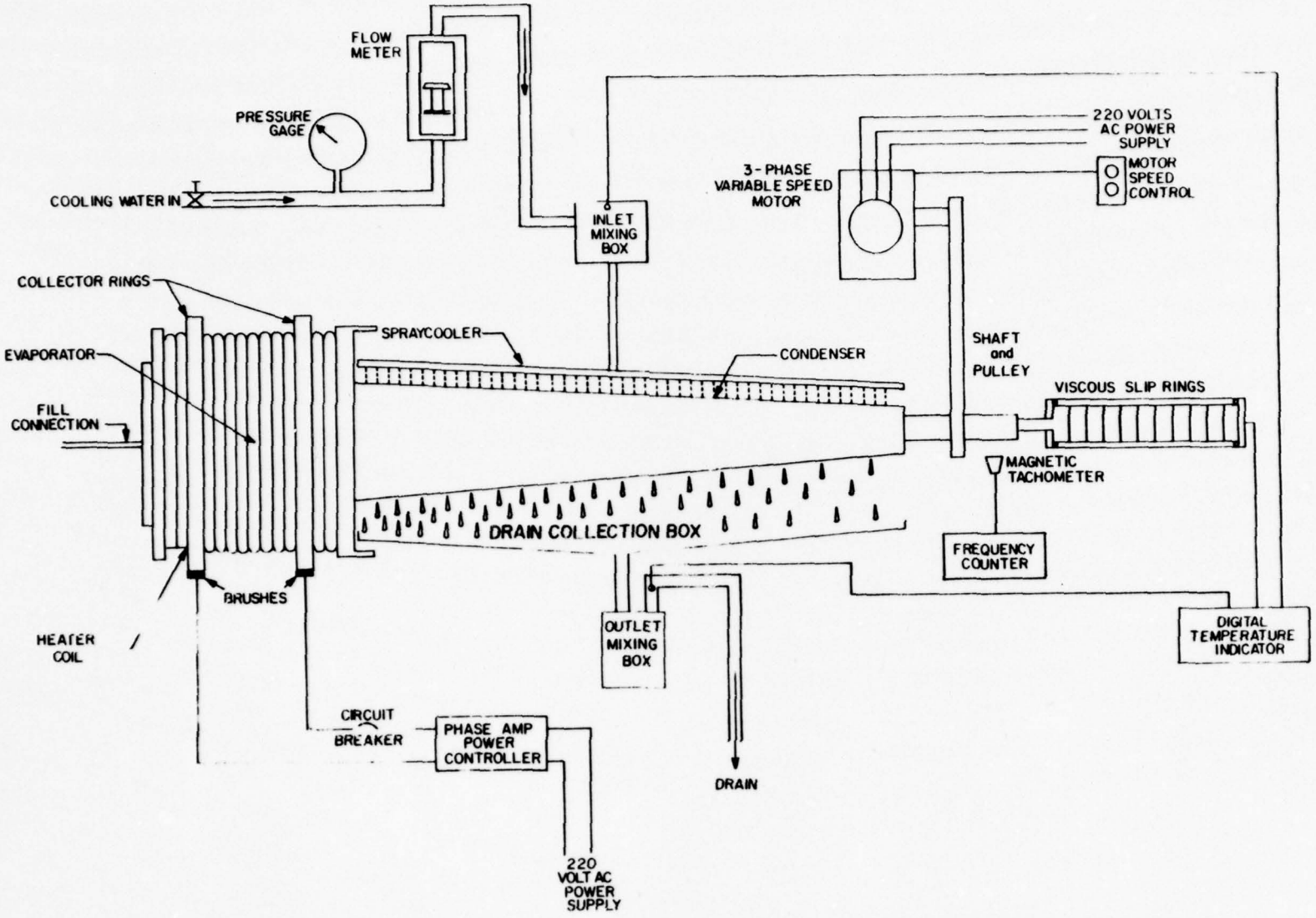

Figure 12. Schematic Diagram of the Heat Pipe Experimental Equipment

III. EXPERIMENTAL PROCEDURE

A. PREPARATION OF THE CONDENSER WALL

Tucker [5] established the procedure for preparation of the copper condenser for obtaining film condensation with water. This procedure was followed, with the modifications listed below:

a. The thermosyphon was tilted so that the evaporator was depressed slightly.

b. The standard cleaning steps were followed except that small quantities of the required solutions were mixed in a 400 ml beaker and the cleaning was accomplished by scrubbing with a bristle brush. By depressing the evaporator end, cleaning fluids were prevented from running back into the heater assembly. Trichloroethane was substituted for trichloroethylene.

c. Complete wetting of the condenser wall was observed after cleaning. The modified procedure was determined to be satisfactory.

The truncated-cone condenser was prepared for dropwise condensation by saturating a swab with n-Octadecyl mercaptan ($C_{18}H_{37}SH$), one percent by weight in Octanoic acid, and thoroughly swabbing the condenser wall. The condenser was rinsed after application of the dropwise promoter and showed no tendency for wetting.

B. FILL PROCEDURES

After completing the above cleaning process, the O-ring and view pieces were installed, and the retainer ring was bolted into place (Figure 5).

The evacuation-fill system, Figure 8, was attached to the 6.0 inch long, 0.25 inch copper fill-tube affixed to the inner view piece. A vacuum was drawn on the system, first with the roughing pump and then with the diffusion pump, keeping valve B closed. A vacuum of 2.0×10^{-5} torr was obtained readily. System integrity was checked by isolating the pump from the system by closing valve A. No change in the mercury column indicated that the system was vacuum tight. Once the system was known to be capable of maintaining a vacuum, with all valves opened, degassing of the working fluid began. The water was degassed for about 30 minutes. Filling was then accomplished by closing valves A and C, picking up and inverting the 1000 ml flask and dumping the water into the heat pipe. Throughout this thesis, 250 ml of distilled water was used as the working fluid. With the water in the evaporator, valve B was closed, and the flask was returned to its holder. The copper tube was then crimped twice with vise grips--once from each side at an angle of about 30 degrees to the axis of the tube. This left a flat section across the tube. At this flat spot the tube was cut with a pair of wire cutters, and the end was covered with a quick-drying epoxy. This procedure was tested with the vacuum system attached to the tube, and no noticeable loss of vacuum was observed after cutting the tube and before applying the epoxy.

C. VENTING PROCEDURES

The venting procedure used by Tucker [5] was followed throughout this thesis. With the heat pipe at a 30 degree angle (evaporator end depressed), power to the heater was set at 0.25 kilowatt. When the saturation temperature in the evaporator was at least 220 degrees Fahrenheit, the vent was opened. The heat pipe was vented for a minimum

of ten minutes to allow escaping steam to drive off any air trapped within the system. The pressure in the heat pipe was maintained above atmospheric pressure by regulating the power to the heater. After venting, the vent and power were secured, in that order.

Excessive power settings during initial venting caused a portion of the polycarbonate view-piece above the level of the water to soften or out-gas to the extent that the view-piece was drawn into the O-ring groove. This created no particular problem but was avoided in subsequent venting operations by keeping the heater power at the 0.25 kilowatt level. Pressure in the evaporator could be maintained acceptably high by regulating the venting with the vent screw rather than by adjusting (specifically, increasing) the power to the heater as above.

D. RUN PROCEDURES

Throughout this thesis, the following running procedure was utilized:

a. Open the cooling water supply valve.

b. Open the bearing cooling water valve.

c. Open the condenser cooling water valve.

d. Adjust the condenser cooling water flow rate to the desired value with the pressure regulator.

e. Open the needle valve on the drop-oiler, permitting one drop every 20-30 seconds to pass into the oil line to the bearing.

f. Start the motor and run the speed up to about 1100 RPM to ensure formation of a liquid annulus in the evaporator.

g. Set the rotational speed to the desired value.

h. Obtain steady-state and take thermocouple readings.

i. Set the heater power to the first level, wait for steady-state and repeat step h.

j. Upon completion of the run at the highest power level (saturation temperature below 212 degrees Fahrenheit), secure the power to the heater and repeat step h.

k. Repeat steps g-j for each of the standard rotational speeds.

E. DATA REDUCTION

Data was reduced by correcting the recorded thermocouple readings to obtain a true reading in millivolts. Correction was accomplished using thermocouple calibration curves. The voltage readings were then converted to degrees Fahrenheit. Cooling water flow rate in percentage flow was converted to pound-mass per hour using the rotameter calibration curve. Using the basic equation

$$Q = \dot{m}C_p\Delta T$$

where $\dot{m}$ = cooling water flow rate, lbm/hr

C_p = specific heat of the cooling water, taken as one BTU per pound-mass per degree Fahrenheit

ΔT = the temperature difference between the cooling water outlet and inlet, °F,

the heat transfer for each power setting was obtained readily. To eliminate the effects of frictional heat generated by the system, the average value of the heat transferred during each of the zero-power runs was subtracted from the heat transferred at any power setting.

IV. PRESENTATION AND DISCUSSION OF RESULTS

A. GENERAL COMMENTS

Throughout this thesis, the term "performance" is used frequently. It is defined as the rate of heat transfer for a given condenser. An "improvement in performance" implies an increased heat transfer rate. Rotational speed is designated RPM. The plots of heat transfer rate versus saturation temperature are referred to as the performance curves. The truncated-cone condenser is referred to as the conical condenser. A run is the accomplishment of steps a-k of the run procedure. Blackened data points represent data taken after, and with the saturation temperature below, the data at the highest saturation temperature. During all runs, the average cooling water inlet temperature was 73 degrees Fahrenheit with a maximum deviation of plus or minus two degrees Fahrenheit.

B. CHOOSING A COOLING WATER FLOW RATE

The cooling system used throughout this thesis was first used by Loynes [6]. He found that to achieve heat transfer rates similar to those of Tucker [5], with the conical condenser, a cooling flow rate of 40 percent was required. Tucker used a spray cooling system and a 30 percent cooling flow rate.

To determine the best flow rate for this thesis, comparative runs were made with the conical condenser at 50 and 70 percent flow rates and 700 RPM. Figure 13 shows the performance of this condenser for these runs. It was clear that the increase in the flow rate from 50 to 70 percent permitted still better performance. However, because maintaining

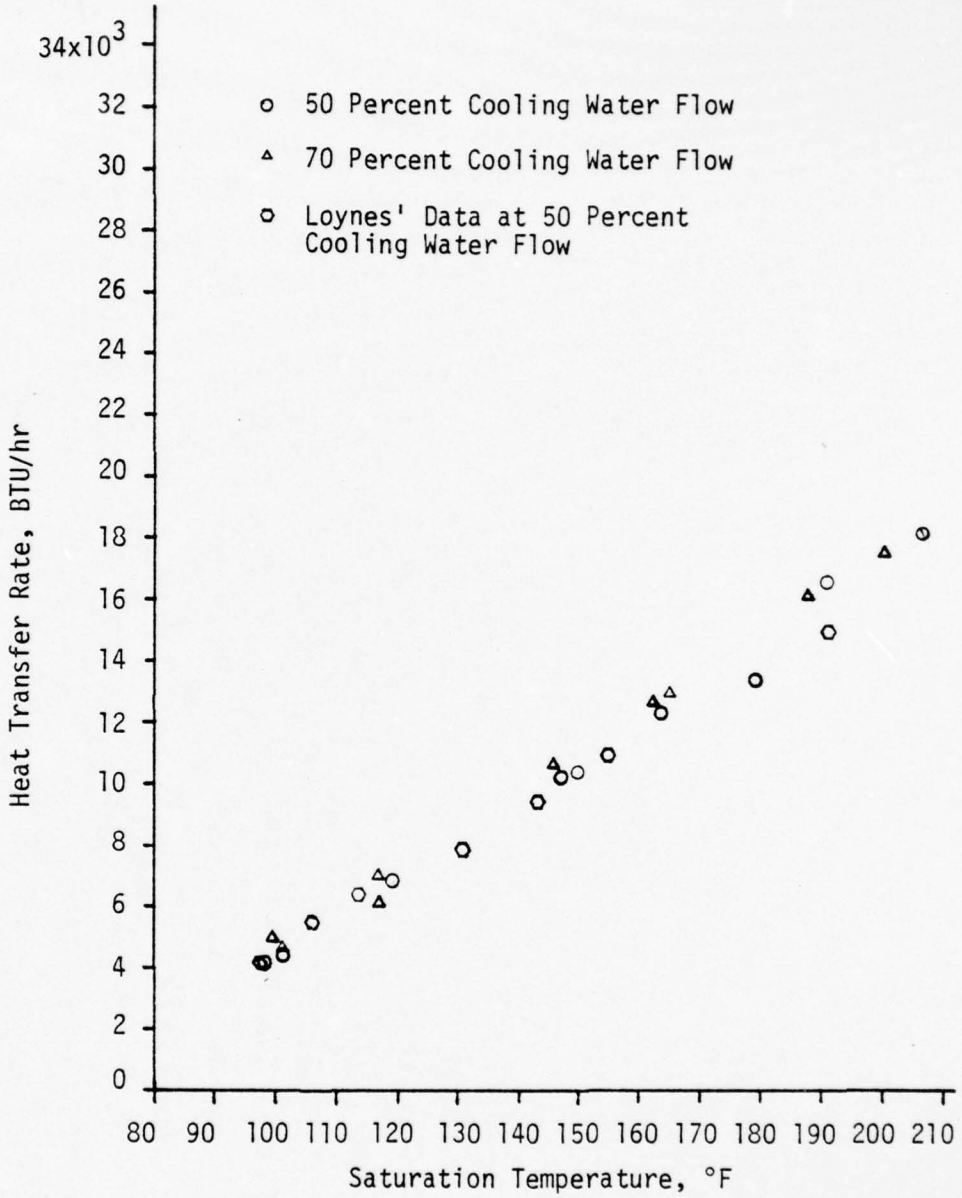

Figure 13. Heat Transfer Rate Versus Saturation Temperature for Truncated-Cone Condenser with Film Condensation at 700 RPM

70 percent coolant flow was difficult during normal working hours, the 50 percent flow rate was chosen as the standard flow rate for this thesis.

Loynes made one run at 50 percent coolant flow rate (700 RPM) with the conical condenser. The results of that run are shown in Figure 13. A comparison of Loynes' data and the two runs of this thesis made under the same conditions showed that very good repeatability was obtainable with this configuration.

Since the initial data correlated well with that of Loynes and showed consistency from run to run, the system was considered ready for use with the 50 percent coolant flow rate as the standard.

C. THE TRUNCATED-CONE CONDENSER

Figure 14 shows the results of the runs made with the conical condenser and film condensation. Performance obviously improves with increasing RPM. This improvement is due to the increased centrifugal force which increases the axial force component on the condensate and thereby increases the condensate flow rate. This increase in working fluid circulation simply means that more vapor can be condensed per unit time. The increase in centrifugal force also flattens the condensate film and thereby reduces the overall thermal resistance in the condenser.

Typical uncertainty limits are shown on Figure 14, calculated as shown in Appendix A.

Figure 15 shows the results of the runs made with the conical condenser prepared to promote dropwise condensation. Performance obviously improved in comparison to the runs with film condensation. This improvement was greatest at 700 RPM and least at 2800 RPM, as can be seen by comparing Figures 14 and 15. The curves for like RPM tend to converge as the saturation temperature increases.

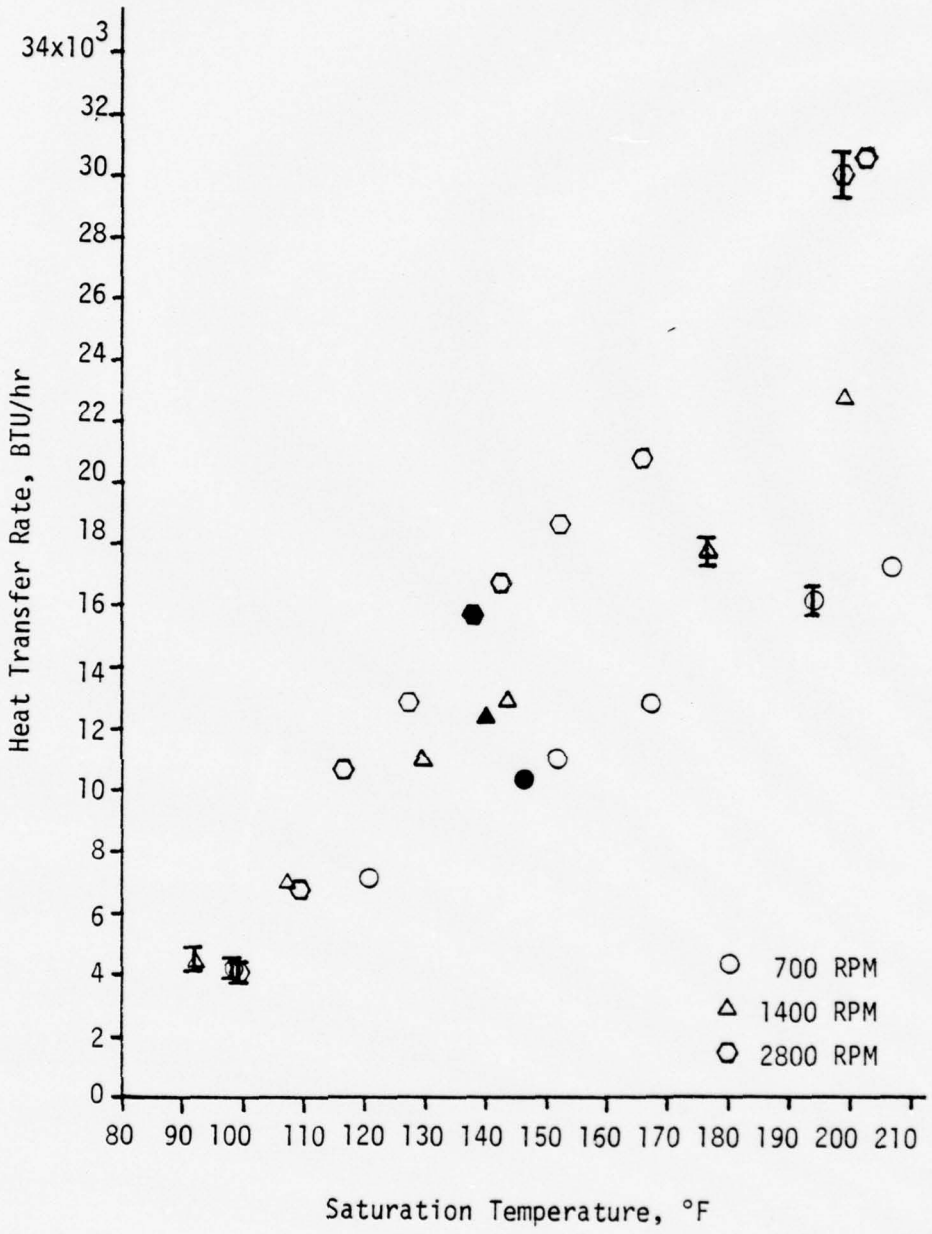

Figure 14. Heat Transfer Rate Versus Saturation Temperature for Truncated-Cone Condenser with Film Condensation (with Typical Uncertainty Limits)

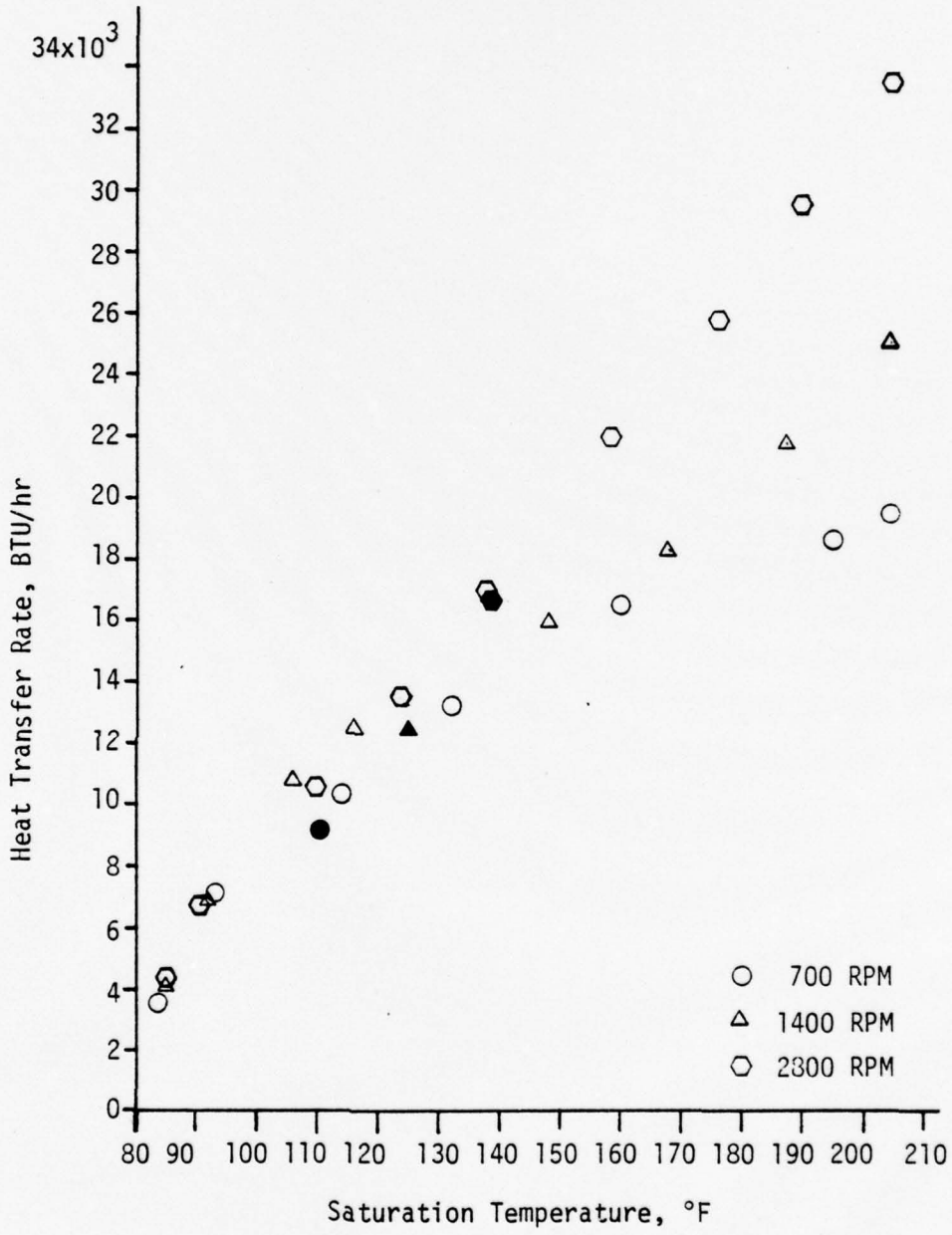

Figure 15. Heat Transfer Rate Versus Saturation Temperature for Truncated-Cone Condenser with Dropwise Condensation

Although visual verification of dropwise condensation was not obtained, the performance indicates that the higher heat transfer rates expected of dropwise condensation (relative to film condensation) were achieved. The decrease in the relative improvement with increasing RPM can be attributed to the decrease in the unwetted condenser wall area due to the effect of the increased centrifugal force on the condensate droplets. The 16 fold increase in this force that occurs when RPM is varied from 700 to 2800 causes increased flattening of the droplets and a tendency toward complete wetting of the wall (film condensation), thereby increasing the overall thermal resistance.

The convergence of the curves at like RPM is probably a manifestation of the effect of the increased internal pressure at these temperatures. Increased pressure has the same effect as increased RPM, which is discussed above.

D. THE 1.00 INCH DIAMETER CYLINDRICAL CONDENSER

This condenser was chosen to provide a base performance to which the internally finned condenser and conical condenser (both of which are more difficult to fabricate) could be compared. It was prepared only for film condensation. Figure 16 shows the performance of this condenser. The heat transfer rate shows the characteristic improvement with increasing RPM. In the case of a rotating cylinder, the condensate flow is induced not by centrifugal force but by a hydrostatic pressure gradient established in the condensate as a result of its variable film thickness. Leppert and Nimmo [7,8] have shown, for this case, that:

$$Nu_m = 0.64Sh^{1/5} , \qquad (1)$$

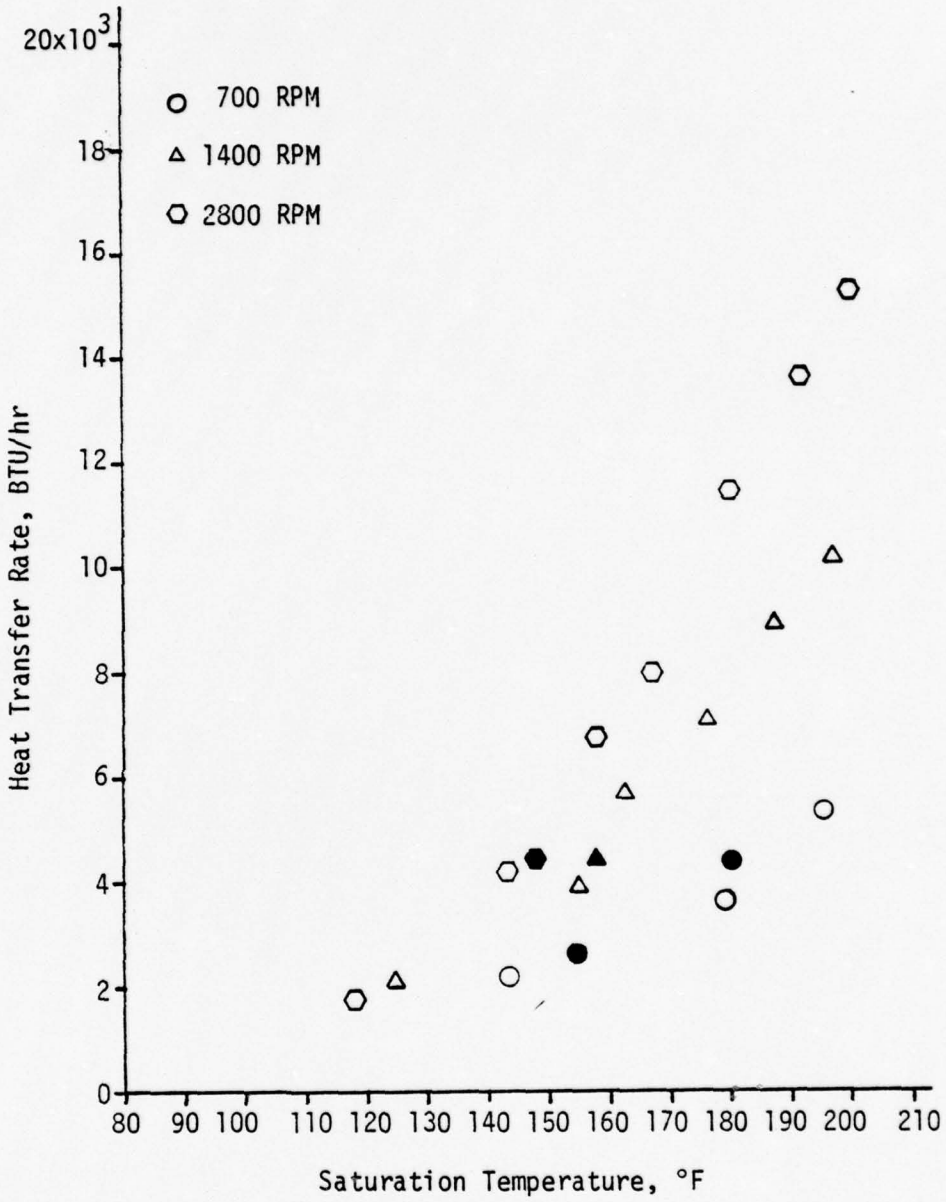

Figure 16. Heat Transfer Rate Versus Saturation Temperature for Cylindrical Condenser, d = 1.00 Inch

where Nu_m = mean Nussult number, hL/k

$Sh = g\rho^2 h_{fg} L^3 / k\Delta T\mu$

g = gravitational acceleration, $\omega^2 R$

ρ = density of condensate

h = average heat transfer coefficient

h_{fg} = enthalpy of vaporization

L = length of condensing surface

k = thermal conductivity of condensate

μ = viscosity of condensate

T = temperature

R = radius of cylinder

This relationship shows that the heat transfer rate for a rotating cylinder increases with increasing RPM, specifically:

$$Nu_m \propto RPM^{2/5} .$$

Based on this proportionality, the performance improvement, as RPM was doubled, was expected to be approximately 30 percent. Figure 16 shows that this improvement was achieved and even exceeded. At the higher saturation temperatures, the magnitude of improvement was approximately 50 percent.

E. THE INTERNALLY FINNED CONDENSER

The internally finned condenser, described earlier, actually had a slightly smaller (unfinned) diameter than the 1.000 inch diameter cylindrical condenser, but the difference (0.001 inch) was considered of no consequence. As seen in Figure 7, the condenser fins are spiraled, having a six inch pitch and counterclockwise twist.

Figure 17 shows the performance of this condenser. Comparison to Figure 16, the performance of the 1.00 inch diameter unfinned condenser, shows that the performance of the finned condenser far exceeds that of the unfinned. The area ratio of the finned to unfinned condenser is 1.64. The fin efficiency is approximately 95 percent. [The performance of this condenser is very nearly equal that of the cone (film condensation). The finned condenser has 100 percent the inner surface area of the cone.]

In addition to the hydrostatic pressure gradient, the forces acting on the condensate included the effect of the spiral fins which imparted a force component parallel to the axis of the condenser. In effect, the spiraling fins served to pump the condensate back to the evaporator. That this occurred was observed during operation - threadlike streams of condensate, flowing over the end of the condenser, could be seen to spiral out rather than follow a radial path.

At the higher saturation temperatures, the internally finned condenser has twice the heat transfer capability of the unfinned condenser. This marked improvement is assumed to be mainly the result of the additional area for heat transfer and perhaps to a smaller extent the pumping action of the spiraled fins, which enhanced condensate flow.

Figure 17 has a gap in the 700 RPM curve. Initially, on the 700 RPM run, no data point was obtained between the saturation temperatures of 158 and 201 degrees Fahrenheit. Nine hours after running this condenser, the heat pipe was well vented (12 minutes) and was run at 700 RPM in an attempt to fill in the gap in the curve. The three data points at 170, 181 and 189 degrees Fahrenheit are the results of this attempt. The prolonged venting should have purged any noncondensible gases that may have entered the system while it was idle. Therefore, data points that

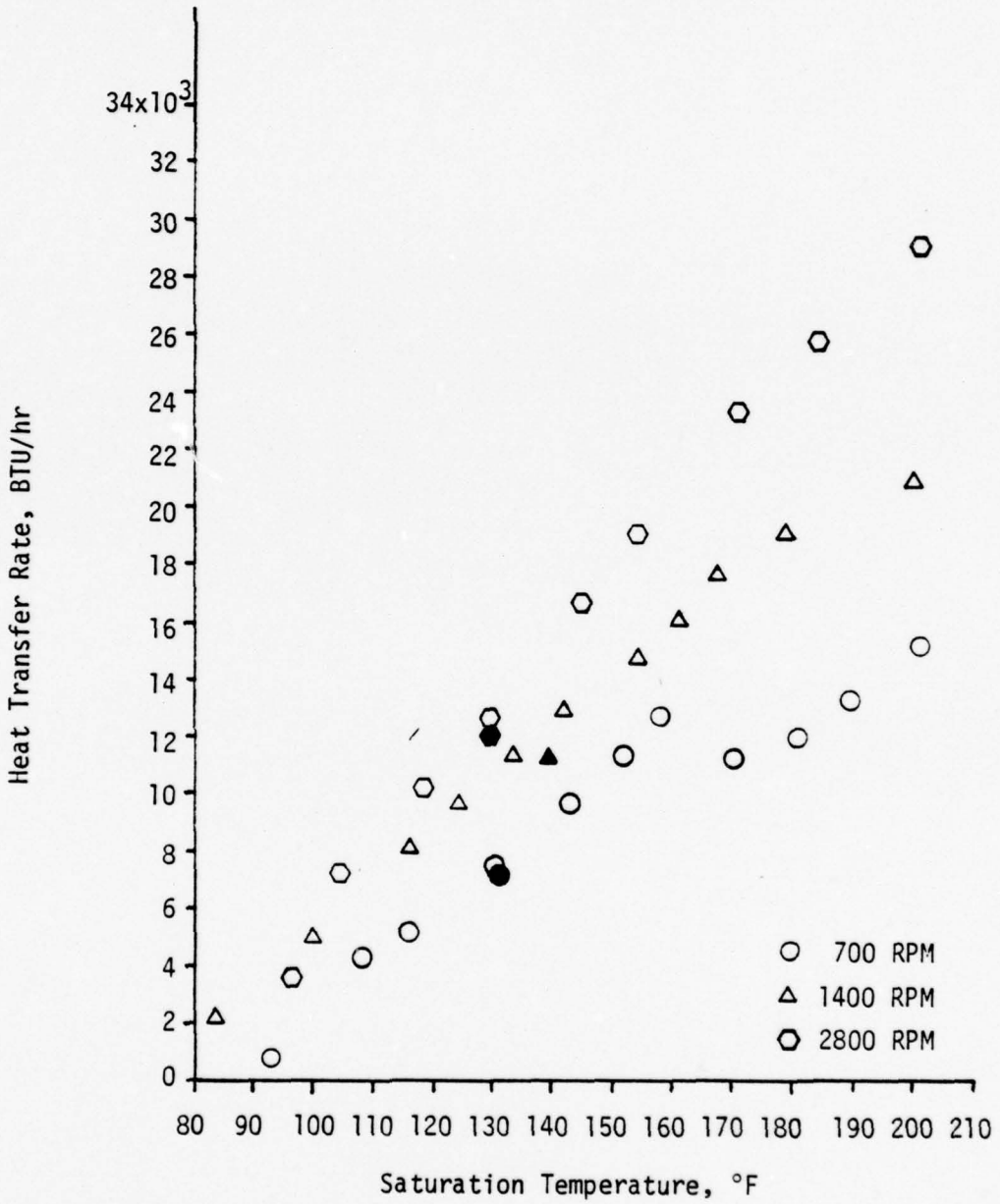

Figure 17. Heat Transfer Rate Versus Saturation Temperature for Internally Finned Condenser

smoothly filled in the curve were expected. The reason that this was not the result is not known. A possible cause is that the polycarbonate end pieces, O-rings and vacuum grease on the O-rings out-gassed during this period such that the thermal resistance was increased. A minor contribution to this nonrepeatability was due to the warmer cooling water (two degrees Fahrenheit). By assuming the original 700 RPM curve to be continuous, the heat transfer rate for saturation temperatures between 160 and 200 degrees Fahrenheit (with cooling water inlet temperature equal that of the first run) can be estimated from the curve. By then substituting the warmer cooling water inlet temperature and recalculating the heat transfer rate, performance can be degraded only about 15 percent (of the assumed original performance). The cause(s) of the remaining discrepancy is not known. Obviously, better repeatability is desired.

Disallowing the gap and the resultant discontinuity in the 700 RPM run, the increase (at a given RPM) in performance appears to decrease with increasing saturation. The slight flattening of the performance curves is evident in Figure 17. The amount of flattening decreases with increasing RPM. No explanation is offered herein for this effect.

F. THE 1.460 INCH DIAMETER CYLINDRICAL CONDENSER

This condenser was designed to permit comparison with the truncated-cone condenser. It was prepared and run only for film condensation. The performance curves are shown in Figure 18 and are intended mainly for comparison to Figure 14.

The curves exhibit the typical trend - improving performance with increasing RPM. As in the case of the smaller cylindrical condenser, condensate flow is induced by the presence of the hydrostatic pressure

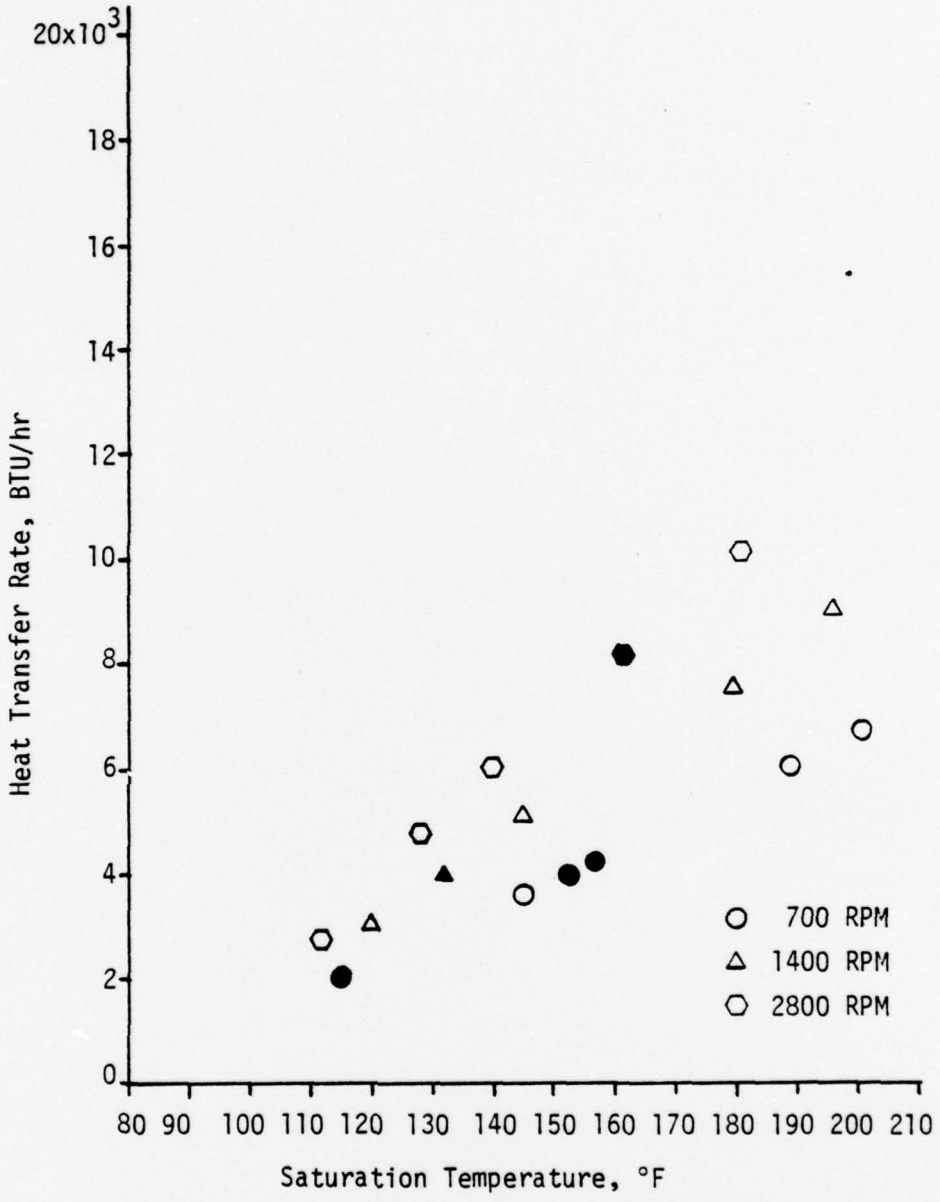

Figure 18. Heat Transfer Rate Versus Saturation Temperature for Cylindrical Condenser, d = 1.460 Inches

gradient. The prediction of improved performance was based on [7]. A 25 percent performance improvement (from one RPM to the next higher at a given saturation temperature) was typical and agrees well with the predicted 30 percent improvement.

The performance of the condenser was very noticeably inferior to that of the conical condenser, as expected. The force component on the fluid, parallel to the wall of the conical condenser and increasing with increasing distance from the end plug, is absent in the cylindrical condenser. Condensate removal is inferior in the cylinder, and this causes the degraded performance. However, the cylinder does permit the transfer of significant amounts of heat and, because of its simple geometry (and therefore low production cost), must not be dismissed for potential applications.

Although not intended as a comparative condenser, the performance of the smaller cylinder was also compared to this condenser. The larger condenser was expected to provide approximately an eight percent performance increase, again based on the work of Leppert and Nimmo [7,8]. The heat transfer rate achieved with the larger condenser was superior to that of the smaller condenser of 700 and 1400 RPM (Figure 16). At the lower saturation temperatures of 2800 RPM, this superiority continued but appears to be lost at saturation temperatures above 170 degrees Fahrenheit. Unfortunately sufficient data was not available at this speed for the larger condenser above saturation temperature of 180 degrees Fahrenheit because of drive motor controller problems at the end of the run.

G. ANALYSIS OF PERFORMANCE OF THE CYLINDRICAL CONDENSER

The performance expectations for the cylindrical condensers were based entirely on the works of Nimmo and Leppert [7,8]. Therefore, to compare the theoretical and empirical results, a log-log plot of the mean Nussult number versus the Sherwood number was made, Figure 19. On this graph, the theoretical relationship expressed by equation (1) was plotted, as shown by the continuous line.

To make the comparison of theoretical versus empirical results, the following simplifications were made:

1. The condenser (outside) wall temperature was taken as the unweighted average of all thermocouple temperatures.
2. All fluid properties were evaluated at the saturation temperature.
3. Heat flux through the condenser was considered uniform.
4. For $\bar{h} = QA/\Delta T$, ΔT was taken as the difference between the saturation temperature and the condenser outer wall temperature.

The mean Nussult number for a given heat transfer rate,

$$Nu_m = \bar{h}L/k = Q/2\pi R\Delta Tk \ ,$$

was determined from the data, and this value was plotted against the corresponding Sherwood number.

Figure 19(a) shows increasing Nu_m with decreasing Sh as ΔT increases. Since this trend is the opposite of what was expected [see equation (1)], the presence of a turbulent type condensate flow was suspected. By the method of Rohsenow and Choi [10], this however was disproved. Calculations showed the condensate film Reynolds number during these tests to be well below the transition value for the appropriate Prandtl number.

The plot of $Nu_m/Sh^{1/5}$ versus the nondimensional quantity $C_p\Delta T/h_{fg}$, Figure 19(b), shows that $Nu_m/Sh^{1/5}$ is not independent of the quantity $C_p\Delta T/h_{fg}$. The exact dependence is, of course, not known.

Although the data points on Figure 19 in general (in their entirety) tend to conform to theory, on a run by run basis substantial disagreement is obvious, particularly for the smaller condenser. The reason for this disagreement is not known at present.

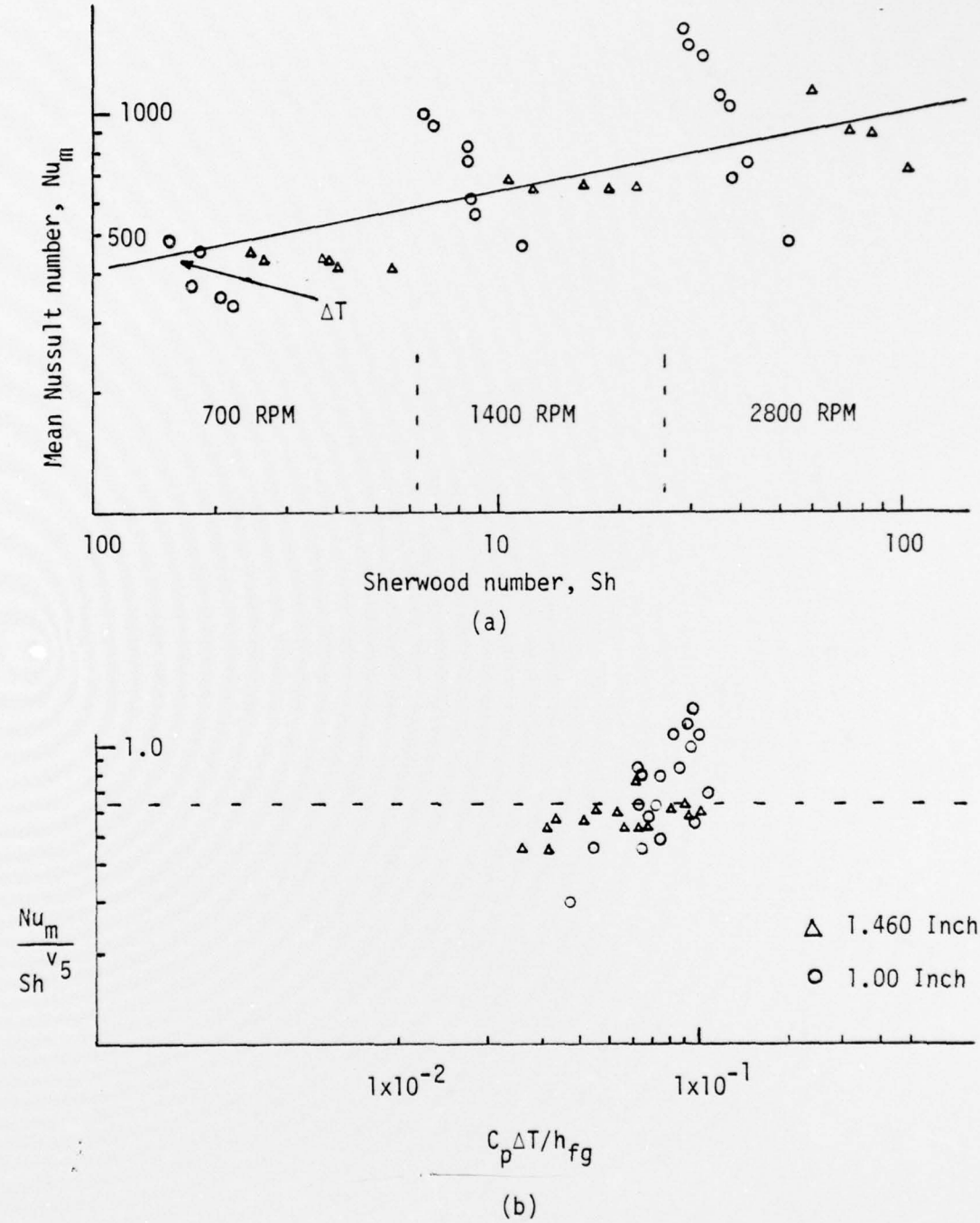

Figure 19(a,b). Analysis of Performance of the Cylindrical Condensers

V. CONCLUSIONS AND RECOMMENDATIONS

A. CONCLUSIONS

Several obvious conclusions can be made based on the experimental results. These are:

1. Dropwise condensation significantly improves performance in the rotating heat pipe with a conical condenser. This improvement is most pronounced at low RPM.
2. A one-degree conical condenser performs better than a cylindrical condenser with a diameter equal to the small diameter of the truncated cone. The conical configuration provides as much as twice the heat transfer capability as the cylinder.
3. The internally finned cylindrical condenser is a dramatic (even exciting) improvement over the smooth-walled cylinder of equal diameter. Heat transfer rates twice as great as with the cylinder were obtained with the finned condenser.
4. For cylindrical condensers, a nearly 50 percent increase in radius provides only minimal increase in the heat transfer capability (less than 10 percent), which is in agreement with predictions based on the work of Leppert and Nimmo [7,8].

B. RECOMMENDATIONS

There are several procedural recommendations relating directly to the NPS heat pipe. These are below:

1. Use only teflon insulated thermocouple wires to minimize breaks in the leads.
2. Periodically grease the Garlock seals to keep coolant water loss to a minimum.

3. Allow a minimum of 10, preferably 15, minutes for the heat pipe to come to steady state at any power setting.
4. Calibrate the coolant water inlet and outlet thermocouples in the ROSEMOUNT oil bath. Obtain as many data points as practical over the operating range of each thermocouple so that uncertainty due to the use of calibration curves can be minimized.

Further experimental work should be conducted with the following condensers:

1. Cylinder with axial fins (no spiral).
2. Finned condensers with dropwise promoter.
3. Truncated-cone with axial fins.

The condenser showing the best performance should be run for a prolonged period, with periods of idleness, and without venting to ascertain the potential for long range (satisfactory) performance. Condensers prepared for dropwise condensation should likewise be run for prolonged periods to determine the long term effect of the presence of the promoter.

The cooling box should be internally divided and separate coolant water discharge lines and thermocouples provided so the heat transfer from finite condenser sections can be measured. This will permit more meaningful theoretical analysis, in that the averaging process will have less pronounced effects on the quantities (dimensional and nondimensional) used in the analysis.

The cylindrical condensers should be run again for prolonged periods. Power level and RPM should be adjusted in order to vary the Sherwood number over a wider range than achieved in this thesis. The smaller condenser should be run particularly carefully in an attempt to reduce the apparent discrepancy between theoretical and empirical performance.

APPENDIX A

UNCERTAINTY ANALYSIS

The uncertainty analysis of the experimental heat transfer rates was by the method of Kline and McClintock [9]. The equations analyzed were:

$$Q_{total} = Q_t = \dot{m}C_p\Delta T_t$$

$$Q_{frictional\ loss} = Q_f = \dot{m}C_p\Delta T_f$$

$$Q_{corrected} = Q_t - Q_f$$

where:

Q_t = total heat transferred to cooling water

Q_f = heat transferred due to friction

Q_c = corrected heat transfer rate

$\dot{m}$ = mass rate of flow of cooling water, lbm/hr

C_p = specific heat of cooling water, BTU/lbm-°F

ΔT_t = difference of cooling water outlet and inlet temperatures, °F

ΔT_f = difference of cooling water outlet and inlet temperatures due to heat of friction, °F

The uncertainties of these quantities are designated:

$$W_Q\ ,\ W_{\dot{m}},\ W_{C_p}$$

The fractional uncertainties are given by:

$$\frac{W_{Q_f}}{Q_f} = \left\{ \left(\frac{W_{\dot{m}}}{\dot{m}}\right)^2 + \left(\frac{W_{C_p}}{C_p}\right)^2 + \left(\frac{W_{\Delta T_f}}{\Delta T_f}\right)^2 \right\}^{1/2}$$

$$\frac{W_{Q_t}}{Q_t} = \left\{ \left(\frac{W_{\dot{m}}}{\dot{m}}\right)^2 + \left(\frac{W_{C_p}}{C_p}\right)^2 + \left(\frac{W_{\Delta T_t}}{\Delta T_t}\right)^2 \right\}^{1/2} .$$

The uncertainty for the corrected heat transfer rate is given by

$$W_{Q_c} = \{W_{Q_t}^2 + W_{Q_f}^2\}^{1/2} .$$

The values and uncertainties of the measured quantities were taken to be

$C_p = 1.000$ BTU/lbm °F

$W_{C_p} = \pm 0.002$ BTU/lbm °F

$\dot{m}$ = 50 percent of maximum flow rate = 1790 lbm/hr

$W_{\dot{m}} = \pm 1$ percent

$W_{T_{in}}, W_{T_{out}} = \pm 0.1$ °F

$$W_{\Delta T} = \{W_{T_{in}}^2 + W_{T_{out}}^2\}^{1/2}$$

For the truncated-cone condenser at 700 RPM the uncertainty analysis is given as

$Q_t = 18491$ BTU/hr

$Q_f = 698$ BTU/hr

$\Delta T_t = 10.33$ °F

$\Delta T_f = 0.39$ °F

$\dot{m}$ = 50 percent maximum flow rate (1790 lbm/hr)

$C_p = 1.00$ BTU/lbm °F

and

$$W_{Q_f} = Q_f \left\{ \left(\frac{W_{\dot{m}}}{\dot{m}}\right)^2 + \left(\frac{W_{C_p}}{C_p}\right)^2 + \left(\frac{W_{\Delta T_f}}{\Delta T_f}\right)^2 \right\}^{1/2}$$

$$= 698 \left\{ \left(\frac{1}{50}\right)^2 + \left(\frac{0.002}{1.000}\right)^2 + \left(\frac{0.14}{0.39}\right)^2 \right\}^{1/2}$$

$$= 698\ (0.360)$$

$$= \pm\ 251 \text{ BTU/hr}$$

$$Q_f = 698 \pm 251 \text{ BTU/hr}$$

$$W_{Q_t} = Q_t \left\{ \left(\frac{W_{\dot{m}}}{\dot{m}}\right)^2 + \left(\frac{W_{C_p}}{C_p}\right)^2 + \left(\frac{W_{\Delta T_t}}{\Delta T_t}\right)^2 \right\}^{1/2}$$

$$= 18491 \left\{ \left(\frac{1}{50}\right)^2 + \left(\frac{0.002}{1.000}\right)^2 + \left(\frac{0.14}{10.33}\right)^2 \right\}^{1/2}$$

$$= \pm\ 253 \text{ BTU/hr}$$

$$W_{Q_c} = \left\{ (W_{Q_f})^2 + (W_{Q_t})^2 \right\}^{1/2}$$

$$= (251^2 + 253^2)^{1/2}$$

$$= \pm\ 356 \text{ BTU/hr}$$

$$Q_c = (18491 - 698) \pm 356 \text{ BTU/hr}$$

$$Q_c = 17793 \pm 356 \text{ BTU/hr}$$

Uncertainties in the heat transfer rates for the truncated-cone condenser, of upper and lower saturation temperatures for each RPM, are plotted on Figure 14 and represent typical performance uncertainties.

APPENDIX B

CALIBRATION OF MEASUREMENT DEVICES

1. Calibration of the Rotameter. The cooling water flow rotameter was calibrated using a Toledo scale, a large container and an electric timer. Calibration proceeded in five percent flow increments from 15 to 90 percent flow rate. Water was collected for as long as 300 seconds at the lower flow rates and for a minimum of 140 seconds at the maximum flow rate. Each flow rate was measured two times. The flow rate (lbm/hr) was plotted versus percent flow through the rotameter. This curve was used to determine mass flow rate for Loynes [6] of 40 percent and this thesis at 50 and 70 percent flow rates.

2. Calibration of the Thermocouples. The thermocouples for the cylindrical and finned condensers were calibrated, prior to installation on the wall, in a ROSEMOUNT variable temperature oil bath utilizing a platinum resistance thermometer as the standard of measurement. They were calibrated as a batch, from 20 to 100 degrees Celsius, in five degree increments. Each thermocouple was separately wired to a channel on the Hewlett Packard data acquisition system and individual readings in millivolts were recorded of each temperature. For each thermocouple the difference Vact-Vi was calculated where:

Vact = reading in millivolts for copper-constantan thermocouple at the temperature of the standard, and

Vi = reading in millivolts for the i^{th} thermocouple at the same temperature.

The mean of these differences was determined and used as the data point for plotting (the correction quantity) $V_{act} - V_{recorded}$ versus thermocouple reading in millivolts at known temperatures. This curve

was used to convert millivolts to temperature for all condenser thermocouples. The maximum difference between the mean and any thermocouple reading was 26 microvolts, about one degree Fahrenheit. This was considered acceptable for the condenser instrumentation.

The thermocouples on the conical condenser and the inlet and outlet thermocouples were calibrated in an insulated, water-filled container. A resistance heater, mixing pump and two quartz thermometers were also placed in the bath. The quartz thermometers had been calibrated separately in the ROSEMOUNT oil bath against the platinum resistance thermometer. All thermocouples were wired to the data recorder. The procedure above was repeated except that averaging was not used in the calibration of the inlet and outlet thermocouples. The thermocouple error $V_{act} - V_{recorded}$ was plotted against millivolts for the thermocouple at the known temperatures.

BIBLIOGRAPHY

1. Daley, T. J., The Experimental Design and Operation of a Wickless Heat Pipe, M.S. Thesis, Naval Postgraduate School, Monterey, California, June 1970.

2. Newton, W. H., Performance Characteristics of Rotating Non-capillary Heat Pipes, M.S. Thesis, Naval Postgraduate School, Monterey, California, June 1971.

3. Woodard, J. S., The Operation of Rotating Non-capillary Heat Pipes, M.S. Thesis, Naval Postgraduate School, Monterey, California, March 1972.

4. Schafer, C. E., Augmenting the Heat Transfer Performance of Rotating, Two-Phase Thermosyphons, M.S.Thesis, Naval Postgraduate School, Monterey, California, December 1972.

5. Tucker, R. S., Heat Transfer Characteristics of a Rotating Two-Phase Thermosyphon, M.S. Thesis, Naval Postgraduate School, Monterey, California, September 1974.

6. Loynes, J. L., Design Improvements on a Rotating Heat Pipe Apparatus, M.S.Thesis, Naval Postgraduate School, Monterey, California, September 1976.

7. Leppert,G., and Nimmo, B., "Laminar Film Condensation on Surfaces Normal to Body or Inertial Forces," Transactions of the ASME, p. 178, February 1968.

8. Nimmo, B. G., and Leppert, G., Laminar Film Condensation on Finite Horizontal Surface, Clarkson College of Technology, Potsdam, New York, 1970.

9. Kline, S. J., and McClintock, F. A., "Describing Uncertainties in Single-Sample Experiments," Mechanical Engineering, p. 3, January 1953.

10. Rohsenow, W. M., and Choi, H., Heat, Mass, and Momentum Transfer, Prentice-Hall, Inc., 1961.

INITIAL DISTRIBUTION LIST

		No. Copies
1.	Defense Documentation Center Cameron Station Alexandria, Virginia 22314	2
2.	Library, Code 0142 Naval Postgraduate School Monterey, California 93940	2
3.	Dr. P. J. Marto, Code 69 Department of Mechanical Engineering Naval Postgraduate School Monterey, California 93940	1
4.	LCDR Lawrence L. Wagenseil USN 20 Helen Drive Dayton, New Jersey 08810	1
5.	Department of Mechanical Engineering Code 69 Naval Postgraduate School Monterey, California 93940	1